LEVEL III

12

MECHANISMS OF CORROSION OF COPPER-NICKEL ALLOYS IN SULFIDE-POLLUTED SEAWATER

Final Report
Covering the Period February 1, 1977 to December 30, 1980

February 1981

By: L. E. Eiselstein, R. D. Caligiuri,
S. S. Wing, and B. C. Syrett

Prepared for:

Office of Naval Research
800 North Quincy Street
Arlington, Virginia 22217

Attention: Dr. Philip Clarkin, Code 471
Director, Metallurgy Program
Materials Science Division

ONR Contract No. N00014-77-C-0046, NR 036-116

SRI Project PYU 6077

SRI International
333 Ravenswood Avenue
Menlo Park, California 94025
(415) 326-6200
Cable: SRI INTL MPK
TWX: 910-373-1246

UNCLASSIFIED

SECURITY CLASSIFICATION OF THIS PAGE (When Data Entered)

REPORT DOCUMENTATION PAGE	READ INSTRUCTIONS BEFORE COMPLETING FORM
1. REPORT NUMBER	2. GOVT ACCESSION NO. AD-A096 865
4. TITLE (and Subtitle) MECHANISMS OF CORROSION OF COPPER-NICKEL ALLOYS IN SULFIDE-POLLUTED SEAWATER	5. TYPE OF REPORT & PERIOD COVERED Final Report, 4 Feb. 1977 to Feb. 1981
	6. PERFORMING ORG. REPORT NUMBER PYU 6077
7. AUTHOR(s) L. E. Eiselstein, R. D. Caligiuri, S. S. Wing and B. C. Syrett	8. CONTRACT OR GRANT NUMBER(s) N00014-77-C-0046/NR 036-116
9. PERFORMING ORGANIZATION NAME AND ADDRESS SRI International 333 Ravenswood Avenue Menlo Park, CA 94025	10. PROGRAM ELEMENT, PROJECT, TASK AREA & WORK UNIT NUMBERS
11. CONTROLLING OFFICE NAME AND ADDRESS Office of Naval Research 800 North Quincy Street Arlington, VA 22217	12. REPORT DATE Feb 1981
	13. NUMBER OF PAGES 78
14. MONITORING AGENCY NAME & ADDRESS (if different from Controlling Office) 12 41	15. SECURITY CLASS (of this report) Unclassified
	15a. DECLASSIFICATION/DOWNGRADING SCHEDULE

16. DISTRIBUTION STATEMENT (of this Report)

Distribution unlimited.

17. DISTRIBUTION STATEMENT (of the abstract entered in Block 20, if different from Report)

18. SUPPLEMENTARY NOTES

19. KEY WORDS (Continue on reverse side if necessary and identify by block number)

Corrosion	Anodic reactions	Corrosion potential
Copper/Nickel alloys	Cathodic reactions	
Seawater	AC impedance	
Sulfide Polluted	Linear polarization	

20. ABSTRACT (Continue on reverse side if necessary and identify by block number)

We have investigated the importance and effects of various variables on the corrosion mechanism of two copper/nickel alloys, CA706 (90%Cu-10%Ni) and CA715 (70%Cu-30%Ni) in seawater. The variables investigated were dissolved oxygen content, sulfide content, pH, flow velocity, sulfide preexposure, various sulfide species, and simultaneous exposure to sulfide and oxygen. The presence of sulfide in seawater was found to prevent formation of the protective corrosion product that normally forms on copper/nickel alloys. Therefore, when both sulfide and oxygen were present in the seawater, the —cont'd

DD FORM 1 JAN 73 1473 EDITION OF 1 NOV 65 IS OBSOLETE

4 1 7 2 7 1

UNCLASSIFIED

SECURITY CLASSIFICATION OF THIS PAGE (When Data Entered)

(Abstract concluded)

corrosion of the alloys was greatly accelerated. A qualitative model was developed to explain the mechanism of uniform corrosion of copper/nickel alloys in various seawater environments.

SUMMARY

This research was stimulated by the premature failure of copper/nickel piping systems in naval vessels being outfitted in a polluted estuary. Specifically, we have investigated the importance and effects of dissolved sulfide pollutants on the corrosion mechanism of two copper/nickel alloys, CA 706 (90% Cu - 10% Ni) and CA 715 (70% Cu - 30% Ni). This final report summarizes the results of the initial research years and describes in detail the progress we have made during the third and final year of this program, in which we concentrated on the CA 706 alloy.

The highlights of our findings in the third year may be summarized as follows.

(1) The corrosion rate of copper/nickel alloys in unpolluted seawater depends strongly on the dissolved oxygen content of the seawater and is controlled by the thickness of a protective inner corrosion product. This corrosion product is most likely composed of Cu_2O doped with small amounts of Fe, Ni, and Cl.

- At low dissolved oxygen levels, the corrosion of Cu/Ni is faster than at intermediate oxygen concentrations because the oxide formed at low oxygen levels does not completely cover the metal surface and therefore is nonprotective.
- At intermediate dissolved oxygen levels, the growth of the Cu_2O corrosion product leads to the establishment of a thick, stable, protective film and a correspondingly low corrosion rate.
- At high dissolved oxygen levels both $Cu_2(OH)_3Cl$ and Cu_2O form. The $Cu_2(OH)_3Cl$ forms at the expense of Cu_2O and therefore the oxide film thickness decreases. Since $Cu_2(OH)_3Cl$ does not form a protective layer, the metal corrosion rate increases significantly.

(2) The addition of sulfide pollutants to nominally deaerated seawater accelerates the corrosion rate of copper/nickel alloys relative to the rate in deaerated, unpolluted seawater. This increase is partly due to the lack of an adherent, protective corrosion product on the metal

exposed to deaerated, sulfide-polluted seawater and partly to the shift of the corrosion potential to values active enough to allow proton reduction as a viable cathodic reaction. However, the corrosion rates of copper/nickel alloys in deaerated sulfide-polluted seawater do not appear to be fast enough to account for the corrosion rates that were observed in the actual polluted estuary environment, ∿ 800 mpy (mils/year).

- The corrosion rate of copper/nickel alloys in sulfide-polluted seawater, either oxygen free or containing only a trace of oxygen, is controlled by the limited amount of either oxygen or hydrogen ions available for the cathodic product. This absence results in the removal of Cu^+ cations from the metal/seawater interface via precipitation of a porous Cu_2S corrosion product. The removal of Cu^+ cations causes the observed active shift in the anodic redox potential.

(3) Copper/nickel specimens preexposed to deaerated, sulfide-polluted seawater corrode faster and take longer for the corrosion rate to decrease in aerated, unpolluted seawater than copper/nickel specimens not preexposed to deaerated, sulfide-polluted seawater. However, even preexposure to sulfide does not seem to account for the corrosion rates measured in the actual polluted estuary environment.

- The corrosion rate of copper/nickel specimens in aerated, unpolluted seawater after exposure to deaerated, sulfide-polluted seawater is high initially because the formation of the protective corrosion product is hampered by the presence of the nonprotective sulfide scale. The gradual replacement of sulfide anions (by oxygen anions) in the porous, nonprotective copper oxide/sulfide scale produces transformation stresses and causes spalling of this scale. The protective Cu_2O corrosion product then forms where the sulfide scale has been removed, resulting in a decrease in the corrosion rate.

(4) Copper/nickel alloy specimens exposed to aerated, sulfide-polluted seawater exhibited the highest measured corrosion rates. These rates are close to those measured in the actual estuary environment. Therefore, the observed accelerated attack of copper/nickel alloy appears to be caused by the <u>simultaneous</u> exposure to dissolved oxygen and sulfide pollutants.

- This accelerated corrosion of copper/nickel alloys exposed first to aerated, unpolluted seawater, then to aerated, sulfide-polluted seawater can be explained

by a twofold effect of sulfide on the protective nature of the preexisting oxide corrosion product. First, the presence of sulfide reduces the Cu^+ ion concentration to extremely low values due to the precipitation of Cu_2S. This leads to a reduction in the anodic redox potential, which not only reduces the corrosion potential but also tends to increase the corrosion rate. Second, at these active potentials, the protective Cu_2O film is thermodynamically unstable and dissolves. The absence of a protective oxide layer results in high corrosion rates in the presence of polluted seawater containing significant levels of oxygen.

TABLE OF CONTENTS

ILLUSTRATIONS

ILLUSTRATIONS (continued)

PREFACE

This report covers the work performed under Contract N00014-77-C-0046, NR 036-116 between February 1977 and February 1981. Listed at the end of the report are the technical papers and technical reports written during the three years of the contract.

The authors would like to thank M.C.H. McKubre for his help with the experiments and their interpretation, B. J. Wood for his work on the Auger electron spectroscopy of the corrosion products, and J. Terry for his work on the scanning electron microscopy and energy dispersive x-ray analysis of the corrosion products. We also thank H. P. Hack of the David W. Taylor Naval Ship Research and Development Center for providing a copper/nickel sample that had been exposed in the James River Test Loop.

I INTRODUCTION AND BACKGROUND

Over the past few years, the U.S. Navy and the public utilities have been supporting research programs to determine the cause or causes of accelerated corrosion of copper/nickel alloys. When these alloys are used for the seawater cooling systems of ships and land-based fossil fuel and nuclear electric power plants,[1,2] they often corrode much faster than expected--up to 800 mpy (mils/year) (H. Hack, private communication). Initial research efforts showed that this accelerated corrosion was related to sulfide pollution in the seawater. Further research was then conducted to determine the corrosion behavior of copper/nickel alloys in various sulfide-polluted seawater environments. The resultant knowledge will help to prevent and control accelerated attack of copper/nickel alloys used in future seawater piping systems.

Copper/nickel alloys are widely used commercially because of their usually good corrosion resistance in seawater environments. The "normal" corrosion resistance (corrosion in unpolluted seawater) of these alloys increases with increasing Ni contents up to about 40% Ni, after which the corrosion resistance remains approximately constant with further Ni additions.[3] This increase in corrosion resistance with increasing Ni contents has been attributed to improved passivation capability[4] and to a beneficial defect structure developed in the Cu_2O upon the addition of Ni.[3] The copper/nickel alloys CA706 and CA715 (90/10 and 70/30 copper/nickel) also contain Fe in solid solution since this alloying addition significantly improves the seawater corrosion resistance. The beneficial effect of Fe has been attributed to the formation of a hydrated Fe oxide in the corrosion product.[5] However, another view is that the addition of Fe changes the Cu_2O defect structure in such a way that Cu_2O doped with Fe will be a better corrosion barrier than undoped Cu_2O.[3]

Several constituents have been identified in the corrosion products of copper/nickel alloys exposed to unpolluted, aerated seawater, but the major constituent is thought to be Cu_2O.[3,6,7] Also varying amounts of $Cu_2(OH)_3Cl$, $Cu(OH)_2$, CuO, $CuCl_2$, $Cu_3(OH)_2(CO_3)_2$ and $CaCO_3$ have been found in the corrosion products of these alloys.[8,9] Ni and Fe have been detected in some of these surface films, and many of the insoluble corrosion products are nonstoichiometric.

Kato et al.[7] described the composition and structure of the corrosion film developed on 90/10 copper/nickel alloys exposed to stagnant aerated 3.4% NaCl solutions. They found that the corrosion film consisted of two layers: a relatively thick porous outer layer composed of mainly $Cu_2(OH)_3Cl$ and a thin inner protective layer composed of Cu_2O highly doped with Cl and Ni. They attribute the good corrosion resistance of this alloy to the inner, thin, protective layer.

The detrimental effect of sulfide in seawater on the corrosion behavior of copper alloys has been known since at least the early 1920s. Bengough and May,[10] with experiments on brass, showed that either CO_2 or H_2S in seawater could be the agent responsible for the transformation of the otherwise protective Cu_2O corrosion product to a nonprotective film. Mor and Beccaria[11] studied the composition of corrosion films developed on copper in deoxygenated synthetic seawater (dissolved oxygen $\leq$ 0.15 ppm) that was polluted with 10 ppm of sulfide. They found that these films contained not only Cu_2O and $Cu_2(OH)_3Cl$, as previously reported for films developed on copper exposed to unpolluted aerated seawater, but also as might be expected, various amounts of CuS and Cu_2S.

Sulfides in seawater result primarily from anaerobic bacteria, which convert the natural sulfate content of the seawater into sulfides. Also, the putrefaction of organic compounds containing sulfur (such as proteins) from sewage treatment plant material contributes to the sulfide content of the seawater. The accelerated attack of copper/nickel alloys was reported[12] as being particularly severe in polluted harbors and estuaries. In these areas the tide changes the seawater from a deaerated, polluted condition to a relatively fresh, aerated condition.

Bates and Popplewell[12] demonstrated that, in deaerated artifical seawater (3.4% NaCl + 0.02% $NaHCO_3$) polluted with 10 g/m^3 (10 ppm)* sulfide, the corrosion rate of 90/10 Cu/Ni and 70/30 Cu/Ni alloys† was relatively low. The corrosion rate was only slightly lower in an aerated unpolluted seawater environment. However, when the alloys were exposed alternately to deaerated sulfide-polluted seawater and then to aerated unpolluted seawater, the corrosion rates observed were significantly higher than those observed either in aerated unpolluted seawater or in deaerated sulfide-polluted seawater.

Gudas and Hack[1] measured the corrosion rates on 90/10 and 70/30 Cu/Ni alloys in aerated natural seawater that was polluted with 0.01 to 0.2 g/m^3 sulfide. They found that these corrosion rates were substantially higher than the corrosion rates measured on the same alloys exposed only to aerated seawater. They reported that the high corrosion rates of the alloys exposed to aerated and sulfide-polluted seawater remained high long after the source of sulfide pollutant was removed.

The precise role of sulfide in the accelerated corrosion of Cu/Ni alloys had not been resolved at the beginning of the present study, even though accelerated corrosion has been reproduced in several investigations.[1,8,12] Also, the environmental and flow conditions considered by these earlier investigations were limited Therefore, the possibility existed that a small change in these conditions could have produced drastically different results than these reported. The effect of these environmental and flow variables on the precise role of sulfide in the mechanism of accelerated attack of Cu/Ni alloys have been studied in greater detail by Syrett, Macdonald, and Wing.[13-20] These authors have considered the effects of dissolved oxygen, dissolved sulfide content,

*1 ppm by weight equals 1 g/m^3. All future concentrations will be given in g/m^3 only.

†90/10 Cu/Ni and 70/30 Cu/Ni will be used to refer to CA 706 and CA 715 copper/nickel alloys, respectively.

seawater velocity, pH, sulfide oxidation products, and sulfide preexposure on the corrosion of Cu/Ni alloys in natural seawater.

The corrosion rate and corrosion potential of Cu/Ni alloys in aerated unpolluted seawater were found[20] to depend on both exposure time and dissolved oxygen (DO) concentrations in the seawater. In general, as the exposure time increases the corrosion rate drops and the corrosion potential rises. The corrosion rate of Cu/Ni alloys generally decreases with increasing oxygen content in the range 0.05 to 6.6 g/m^3. In seawater containing 26.3 g/m^3 oxygen, a further decrease in corrosion rate was observed for 90/10 Cu/Ni alloy for exposure periods up to 100 hr, but a slight increase was observed after a 200-hr exposure. Increasing the oxygen content from 6.6 to 26.3 g/m^3 caused a marked increase in the corrosion rate of 70/30 copper/nickel alloy for exposure periods greater than 50 hr. Corrosion potentials increased with increasing oxygen concentration in the range 0.85 to 26.3 g/m^3. When the oxygen content was reduced from 0.85 to $\leq$ 0.045 g/m^3, corrosion potentials rose slightly (90/10 Cu/Ni) or significantly (70/30 Cu/Ni) for reasons that were not determined.

To determine the effect of sulfide on the corrosion of copper/nickel alloys, Macdonald, Syrett, and Wing[14,18] monitored the corrosion rates of the copper/nickel alloys in deaerated seawater containing 0-55 g/m^3 sulfide and flowing at 1.62 m/s. In unpolluted deaerated seawater, the corrosion rates were extremely low because the cathodic reaction was limited to the reduction of the trace amounts (< 0.5 g/m^3) of dissolved oxygen present. On the other hand, corrosion rates in sulfide-polluted deaerated seawater were much higher because an active shift in the corrosion potential allowed hydrogen ion reduction to become an active cathodic process. However, the corrosion rates in sulfide-polluted deaerated seawater were not high enough to account for the accelerated attack noted[21] in the seawater piping of naval ships. Indeed, the results were consistent with those of Bates and Popplewell[12] in that corrosion rates in sulfide-polluted deaerated seawater were of the same order as those obtained in unpolluted aerated seawater.

Syrett and Wing[7] then considered the possibility that sulfide-polluted deaerated seawater could cause accelerated attack if the flow conditions were sufficiently adverse. A comparison of corrosion rates in unpolluted aerated seawater and in deaerated seawater containing about 0.2 g/m^3 sulfie indicated that, even at velocities as high as 5 m/s, the corrosion rates in the polluted environment were less than in the unpolluted seawater.

Syrett[13] considered the possibility that sulfide-polluted, deaerated seawater could cause accelerated attack if the pH of the deaerated seawater was decreased at the same time that the seawater was polluted with sulfide. This experiment demonstrated that Cu/Ni alloys do not suffer accelerated attack at a flow velocity of 3 m/s in sulfide-polluted deaerated seawater even when the pH is allowed to drop to values as low as 7.

The accelerated attack of copper/nickel alloys could result from contact with sulfide oxidation products rather than from contact with the sulfide or oxygen from which they were derived. To test this hypothesis, Syrett, Macdonald, and Wing[15] performed rotating cylinder experiments in seawater that contained oxygen, sulfide, sulfur, and polysulfide, either singly or in combination. The test period was fairly short (about one day), and the corrosion rates were measured only semiquantitatively (by the polarization resistance technique). Nevertheless, these experiments demonstrated that sulfur or polysulfides were just as effective as sulfide in promoting corrosion in deaerated seawater but that, compared with oxygen (in aerated seawater), none of the sulfur-containing species caused dramatic increases in the corrosion rate.*

The presence of the sulfur species, however, did have a profound effect on the character of the surface film. The cuprous oxide films formed during the one-day exposure to unpolluted seawater were relatively smooth

*If the tests had been run for longer times, it is possible that differences between the corrosivity of the various sulfide species would have eventually emerged.

and nonporous, while the sulphur-containing films, presumed to be substoichiometirc forms of cuprous sulfide,[14] were relatively thick and porous. It was speculated[15] that the presence of sulfide (or some sulfide oxidation product) does not lead directly to accelerated corrosion; rather, the porous sulfide corrosion product formed in the polluted seawater interferes with the normal growth of the protective oxide film on subsequent exposure to unpolluted seawaters. The results of subsequent sulfide exposure experiments[13] indicated that this was true. A sulfide-containing corrosion film was formed upon exposure of the alloy to deaerated, polluted seawater. When this Cu/Ni alloy was later exposed to aerated, unpolluted seawater, the sulfide-containing corrosion product interfered with the formation of the normally protective oxide film. The corrosion rates did not decrease rapidly for Cu/Ni alloys preexposed to sulfide, as was the case for Cu/Ni alloys not preexposed to sulfide. Instead the corrosion rates remained high for several days after exposure to unpolluted aerated seawater.

The corrosion rate data collected shortly after exposing sulfide-preexposed Cu/Ni alloys to aerated seawater failed to indicate whether or not the corrosion rate of sulfide-preexposed specimens was initially higher than that of "fresh" specimens. In the third year of the present program an attempt was made to answer this question. Furthermore, besides verifying the effect of sulfide preexposure on corrosion rates, the present set of experiments was designed to evaluate the effect of sulfide-polluted and aerated seawater on the corrosion behavior of Cu/Ni alloys.

II MATERIALS AND EXPERIMENTAL METHODS

Materials

Seawater

Filtered natural seawater was obtained from the Steinhart Aquarium, San Francisco, and was used as the corrosive medium in all the experiments reported in this study. The properties of this seawater were as follows:

Salinity	24 g/m^3
Density	1.0214 g/cm^3
Turbidity	0.2 Jackson
pH	8.2 $\pm$ 0.10

The seawater was collected in polyethylene-lined 0.21-m^3 (55-gallon) drums and was continuously purged with air to inhibit growth of anaerobic organisms during storage.

The pH of the seawater was monitored at regular intervals during the experiments. The pH varied from about 7.80 to 8.30, which is within the normal range for fresh or polluted seawater. Syrett[13] has shown that this variation in pH does not significantly affect the corrosion of Cu/Ni alloys in deaerated, sulfide-polluted seawater.

During part of the test, the seawater was sparged continuously with air; dissolved oxygen levels in this aerated environment (henceforth termed A-seawater) were typically 6.6 g/m^3 as measured using either the Winkler titration method[22] or the Chemetic Colormetric test. This value is consistent with those reported by others.[23] In another part of the test, deaerated, sulfide-polluted seawater (henceforth termed DS-seawater) was required. In preparation of this environment, the seawater was first sparged with nitrogen to reduce oxygen levels to 0.05 g/m^3, but as discussed later, it is likely that this low oxygen content was not maintained during testing and that values rose to 0.1 g/m^3 or higher.

In a third part of the test, air was intentionally allowed to be drawn into the flow system to produce an aerated, sulfide-polluted seawater (henceforth termed AS-seawater); here, oxygen levels could not be closely controlled, but chemical analysis by the Chemetic Colormetric test indicated oxygen contents of 0.2 ± 0.1 g/m^3. Because oxygen may have been reduced by the dissolved sulfide during the period of sampling and titration, it is conceivable that oxygen contents in AS-seawater were somewhat higher than those reported.

Preliminary experiments indicated that it is difficult to maintain tight control of the sulfide level in the recirculating seawater loop by sparging with a nitrogen/hydrogen sulfide gas mixture because sulfide consumption varies with the test specimen exposure time and with the dissolved oxygen in the seawater. In the present set of experiments, a 0.1 molar solution of Na_2S in deaerated seawater was used to control the sulfide level in the DA-seawater and AS-seawater. The dissolved sulfide was then analyzed by a $Pb(ClO_4)_2$ titration, using an Orion sulfide-selective electrode to detect the end point. The sulfide level was analyzed at least four times a day and was controlled at 1.00 ± 0.60 g/m^3 in AS-seawater and at 0.75 ± 0.55 g/m^3 in DS-seawater.

Copper/Nickel Alloys

In the first two years of this program, both 90/10 Cu/Ni and 70/30 Cu/Ni were studied. However, in the experiments of the third year reported here, only one Cu/Ni alloy could be studied because ten replicate specimens were needed and each of the two available test channels on the recirculating flow loop could accomodate only five specimens. The 90/10 Cu/Ni alloy was chosen over the 70/30 alloy because most premature failures on naval ships have occurred in seawater piping of this composition (H. P. Hack, private communication, 1978).

The 90/10 Cu/Ni alloy (supplied by Anaconda Company, Brass Division, Paramount, CA) had a yield strength of 148 MPa and a tensile strength of 319 MPa. Optical metallography revealed the microstructure to consist of equiaxed grains 15 to 20 μm in diameter, and an occasional twin. No unusual defects or microstructures were observed. The chemical composition (in weight %) is listed below:

Cu	87.9	P	$\leq$ 0.02
Ni	10.2	Pb	0.010
Mn	0.24	S	$\leq$ 0.02
Fe	1.34	Zn	0.28

Tubular specimens of the 90/10 Cu/Ni alloy were cut from annealed tubing in lengths of 2.54 cm. The inner and outer diameters of the tubing were 1.35 and 1.71 cm, respectively. The surfaces of the specimens were degreased in acetone, descaled in a HCl/H_2SO_4 solution (ASTM Recommended Practice G1-72 for copper alloys), rinsed with methyl alcohol, rinsed with deionized water, and then dried in warm air. The specimens were weighed to within 0.1 mg immediately before the test loop was started.

Methods

Description of Recirculating Flow Loop

The recirculating flow loop used in this work is shown schematically in Figure 1. A titanium heat exchanger was needed to remove the heat supplied to the flowing seawater by the pump. The temperature of the seawater was maintained at 23.2 $\pm$ 1.3°C throughout the experiment. Soluble titanium species were not detected in the seawater, at least down to the detection limit of 10 g/m^3. One of the rotameters was fitted with a stainless steel float, but periodic chemical analysis indicated that soluble iron species were not present, at least down to the detection limit of 0.1 g/m^3. Except for the Cu/Ni test channels, all other components of the system were either plastic or glass.

The seawater velocity in the test channels could be varied between 0.5 and 5 m/s by adjusting the valve in the velocity-control bypass loop shown in Figure 1. These flow velocities are equivalent to Reynolds numbers of 7,400 to 74,000 for our specimen size and flow geometry. All tests were maintained at a flow velocity of 3 m/s corresponding to a Reynolds number of about 44,000.

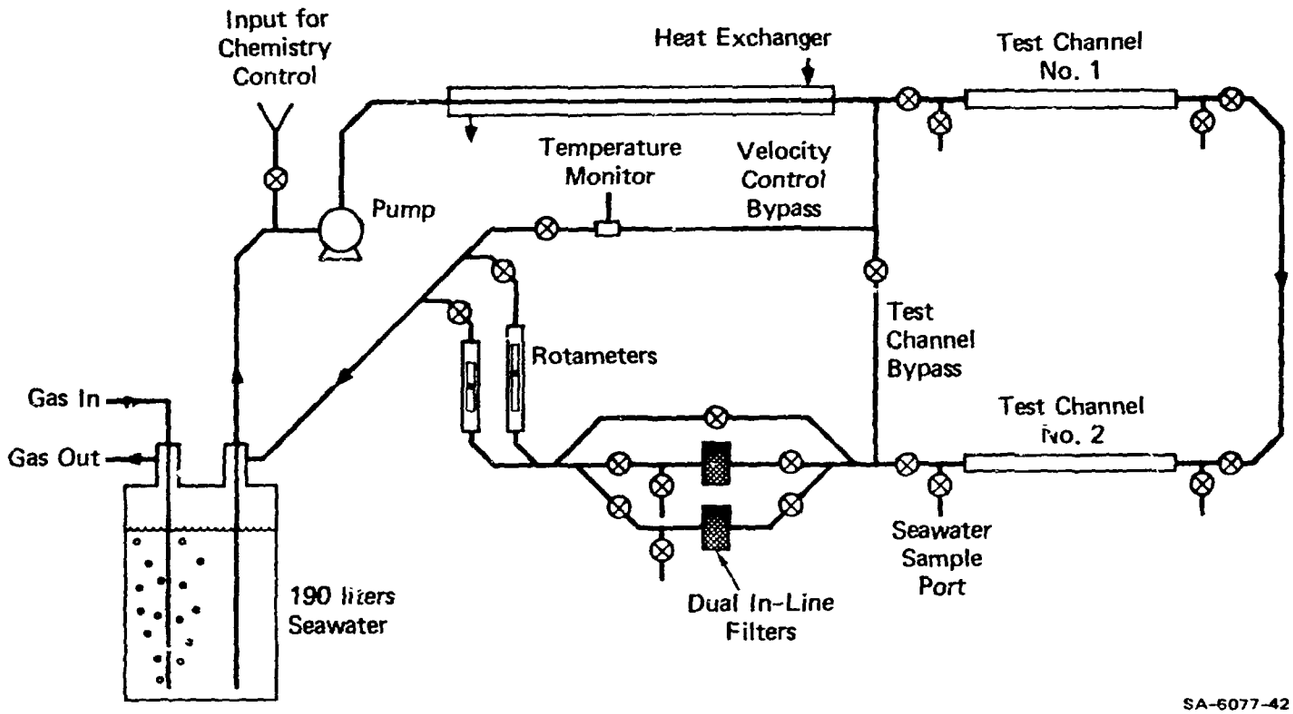

FIGURE 1 SCHEMATIC DIAGRAM OF THE FLOW LOOP

Details of the test channel are shown in Figure 2. The five 2.54-cm lengths of cleaned and annealed 90/10 Cu/Ni tubing were physically and electrically separated by Delrin spacers, and clamped tightly together with four bolts. The seawater was pumped through the two test channels in series. Each test channel contained a 70-cm-long 90/10 Cu/Ni tubular approach section in front of the specimen assemblies. Electrochemical measurements were facilitated by connecting an electrolytic bridge to a saturated calomel reference electrode (SCE) immediately upstream from each test section. The 90/10 Cu/Ni tubular approach section served as the counterelectrode.

Specimen Exposure Histories

The test loop was run with ten 90/10 Cu/Ni specimens for a total time of approximately 41 days. The various seawater environments (described previously) were used in sequence as follows: (1) DS-seawater for 4 days, (2) A-seawater for 16 days, (3) AS-seawater for 6 days, and (4) A-seawater for 15 days. At periodic intervals during the 41-day exposure, specimens were removed for scanning electron microscopy (SEM) and gravimetric measurements and replaced with fresh, unexposed specimens. This periodic removal could be done quickly and without unduly affecting the seawater chemistry or perturbing the remaining specimens. However, no specimens were replaced during the DS-seawater phase of the test cycle to minimize the chance of introducing excessive amounts of oxygen into the system. The specimen replacement technique allowed the comparison of specimens subjected to a variety of exposure histories.

Gravimetric Corrosion Measurements

Gravimetric measurements were performed on a few specimens. The procedure outlined in ASTM G1-X2-72 was used to determine the weight loss from corrosion.[24] This procedure is used to measure weight loss when the solution for removing corrosion products also attacks the base metal. The solution used in this study contained 500 ml HCl, 100 ml H_2SO_4, and water to make 1 liter. The mass loss from corrosion can be determined to within an accuracy of $\pm$ 1.0 mg by this method.

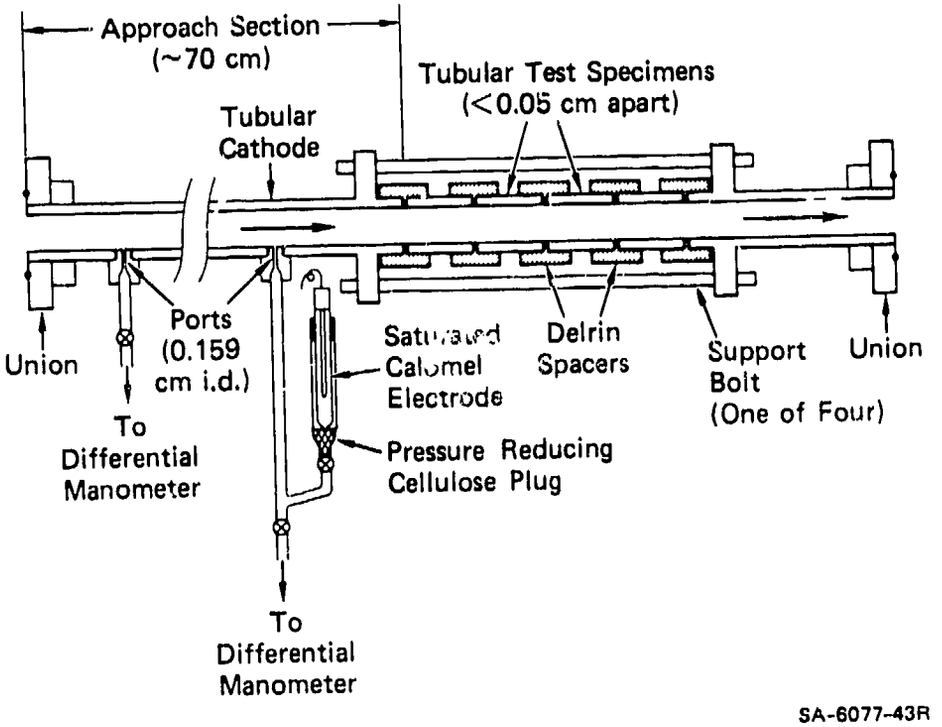

FIGURE 2 DESIGN OF TEST CHANNEL

Electrochemical Corrosion Measurements

The use of electrochemical techniques for measuring corrosion rates of metals in condensed media is well established.[25,26] The most frequently used technique involves measurement of the polarization resistance at the metal/solution interface. The calculated polarization resistance of the corroding interface can then be related to the rate at which the interface is corroding.[23,27,28] This relationship is discussed in more detail in the Appendix.

In this experiment both linear polarization and ac impedance were used to determine the polarization resistance at the metal/solution interface. The linear polarization technique was used to determine the polarization resistance of the corroding specimens by measuring the current and potential changes when the specimen is cyclically polarized by imposing a 6-mV (vs SCE) peak-to-peak triangular voltage excitation across the specimen/seawater interface using a potentiostat and function generator. The apparent polarization resistance (R_a) was determined at several potential sweep rates in the range 0.01 to 1.0 mV/s, and the "true" polarization resistance (R_p) was determined by plotting $\frac{1}{Ra}$ versus the potential sweep rate and extrapolating to zero sweep rate.[28]

The ac impedance was measured using both potentiostatic and galvanostatic control. However, most of the measurements were done in galvanostatic control. The general layout of the electronic components employed is similar to that described in the literature.[25] The real and imaginary components of the complex impedance were measured as a function of frequency using a potentiostat and a Solartron impedance meter. A 20-μA peak-to-peak sine wave excitation was applied across the interface, and the frequency was varied from 10^{-3} to 9.99×10^{3} Hz.

Corrosion potentials for both methods were monitored throughout the test period with respect to a saturated calomel electrode (SCE).

III EXPERIMENTAL RESULTS

Corrosion Potential Measurements

The measured corrosion potentials of the 90/10 Cu/Ni alloy and corresponding seawater chemistries are plotted as a function of time in Figure 3. The corrosion potentials in DS-seawater, Figure 3(a), varied from -0.45 to -0.70 V (SCE). These potentials are somewhat higher than those previously reported[13,15] and indicate that some oxygen (perhaps 0.1 g/m^3) was present in this environment.

The corrosion potentials measured on the Cu/Ni specimens exposed to A-seawater, Figure 3(b) and (d), were more noble, with the potentials varying from -0.05 to -0.10 V (SCE). The corrosion potentials in AS-seawater, Figure 3(c), varied between -0.60 and -0.20 V (SCE) and seemed to be dependent on the sulfide concentration. When the sulfide was added to the loop, the corrosion potential dropped to about -0.60 V (SCE). As the sulfide was oxidized, the potential slowly increased to a maximum of about -0.20 V (SCE). Exposure history was found to have only a small effect on the corrosion potential. These corrosion potential data are in good agreement with previous work.[13-20]

Tafel Coefficient Measurements

The relationship between the polarization resistance and the corrosion rate is discussed in the Appendix. As shown in Equation (A7), the instantaneous corrosion current is proportional to the reciprocal of the polarization resistance ($1/R_p$) and can be calculated if the Tafel coefficients are known. The instantaneous corrosion rate can then be calculated from the instantaneous corrosion current, as shown in Equation (A10). Determination of the Tafel coefficients involves measuring the current/voltage response when the specimen potential is shifted far from the corrosion potential in both the active and noble directions.

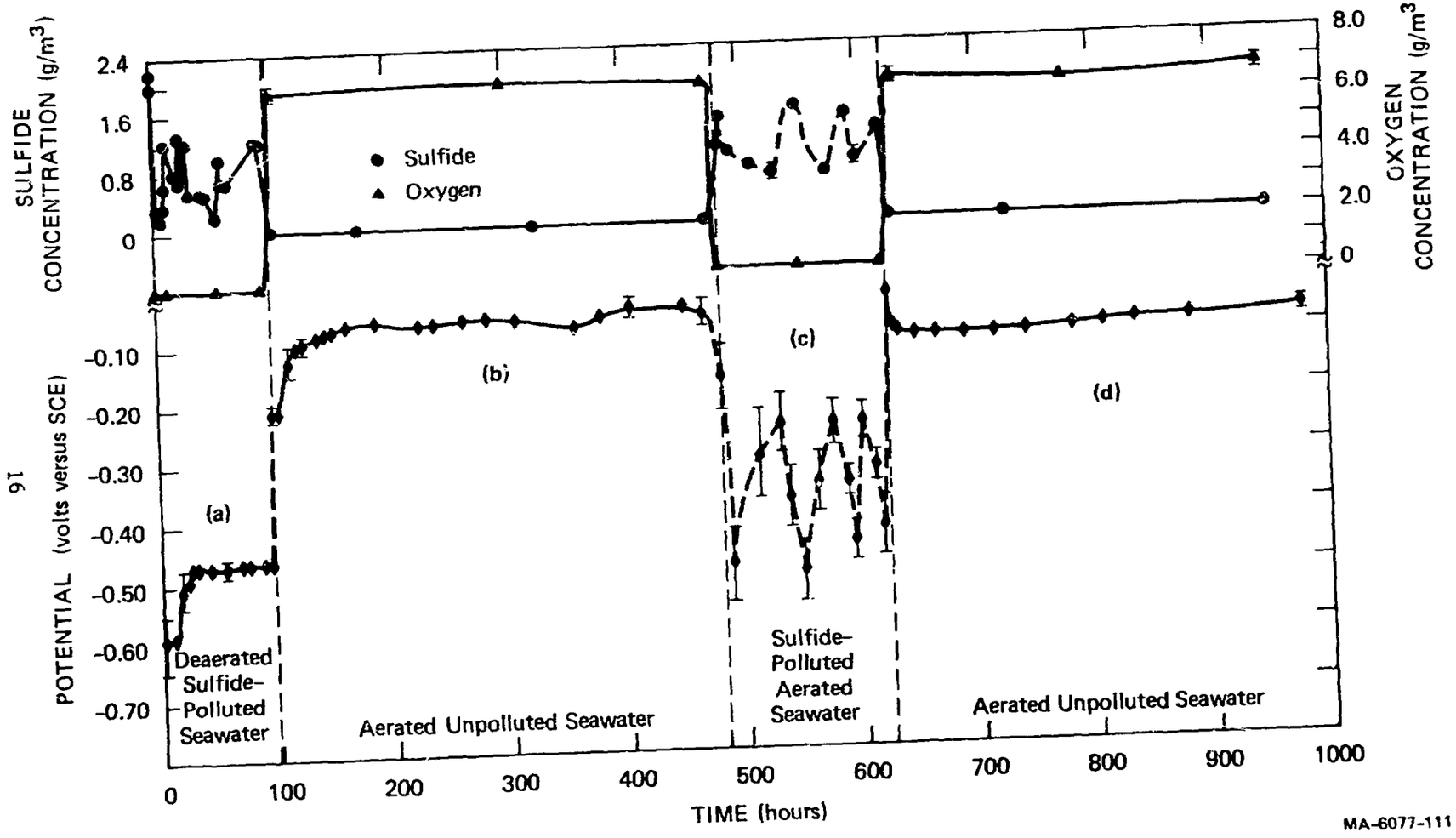

FIGURE 3 POTENTIAL-TIME CURVE FOR 90/10 COPPER/NICKEL ALLOY IN FLOWING SEAWATER WITH ASSOCIATED OXYGEN AND SULFIDE EXPOSURE HISTORIES

(pH = 8.1 ± 0.2, Temperature = 23.2 ± 1.3°C, Reynolds Number ≅ 44,000)

This large polarization, usually > 20 mV, disturbs the corrosion product film. Therefore, specimens that are used for Tafel coefficient measurements cannot be used for linear polarization, ac impedance, gravometric, or film characterization studies. Since the seawater loop can only hold 10 specimens at one time, comparatively few Tafel coefficient measurements were made. The results are reported in Table 1. A typical example of the polarization versus logarithm of the current density data used for the Tafel coefficient determinations is shown in Figure 4. It is recognized that Tafel coefficients measured from such curves can be only approximate, but care was taken to make all measurements internally consistent and comparable.

The anodic and cathodic Tafel coefficients (λ_1 and λ_2, respectively) seem to be relatively independent of the environment or the specimen exposure history. The Stern-Geary coefficients $[\lambda_1\lambda_2/(\lambda_1 + \lambda_2)]$ used to convert the linear polarization resistance into corrosion rate are also reported in Table 1 for each test condition. The Stern-Geary coefficients also do not change drastically with environment or exposure history. However, the specimens exposed to AS-seawater have the highest coefficients ($\sim$ 40 mV), while specimens exposed to DS-seawater have the lowest coefficients ($\sim$ 20 mV). The Stern-Geary coefficients measured on specimens exposed to A-seawater also showed some variation with sulfide preexposure history. The coefficients, were higher for sulfide-preexposed samples ($\sim$ 38 mV) and lower for samples that were never exposed to a sulfide-containing environment.

Corrosion Rates as a Function of Exposure History

The Tafel coefficients were used to obtain corrosion rates from the polarization resistance measurements using the method discussed in the Appendix. Note that the error in the corrosion rates obtained by this method is likely to be $\pm$ 30% of the reported value and could, in fact, be substantially higher. Nevertheless, since all measurements and calculations were performed in a uniform fashion, it is to be expected that the corrosion currents reported are directly comparable with one another.

Table 1

TAFEL COEFFICIENTS, STERN-GEARY COEFFICIENTS, AND CORROSION POTENTIALS OF Cu/Ni ALLOYS IN VARIOUS SEAWATER ENVIRONMENTS

Preexposure*	Test Environment*	Tafel Coefficients (mV) Anodic	Tafel Coefficients (mV) Cathodic	Stern-Geary Coefficient (mV)	Corrosion Potential E_{corr} (mV)
AS-seawater, 6 days	A-seawater, 185 hr	76	80	39	-107
DS-seawater, 4 days; A-seawater, 16 days; AS-seawater, 6 days	A-seawater, 185 hr	74	68	35	-94
A-seawater, 16 days	AS-seawater, 6 days	78	78	39	-438
None	AS-seawater, 6 days	78	82	40	-443
DS-seawater, 4 days; A-seawater, 6 days	AS-seawater, 6 days	80	69	37	-442
None	A-seawater, 5 days	54	36	22	-85
DS-seawater, 4 days	A-seawater, 16 days	65	44	26	-72
DS-seawater, 4 days	A-seawater, 4 hr	73	89	40	-211
None	A-seawater, 4 hr	77	52	31	-228
None	DS-seawater, 92 hr	45	30	18	-455

*DS-seawater = deaerated, sulfide-polluted seawater.
A-seawater = unpolluted, aerated seawater.
AS-seawater = aerated, sulfide-polluted seawater.

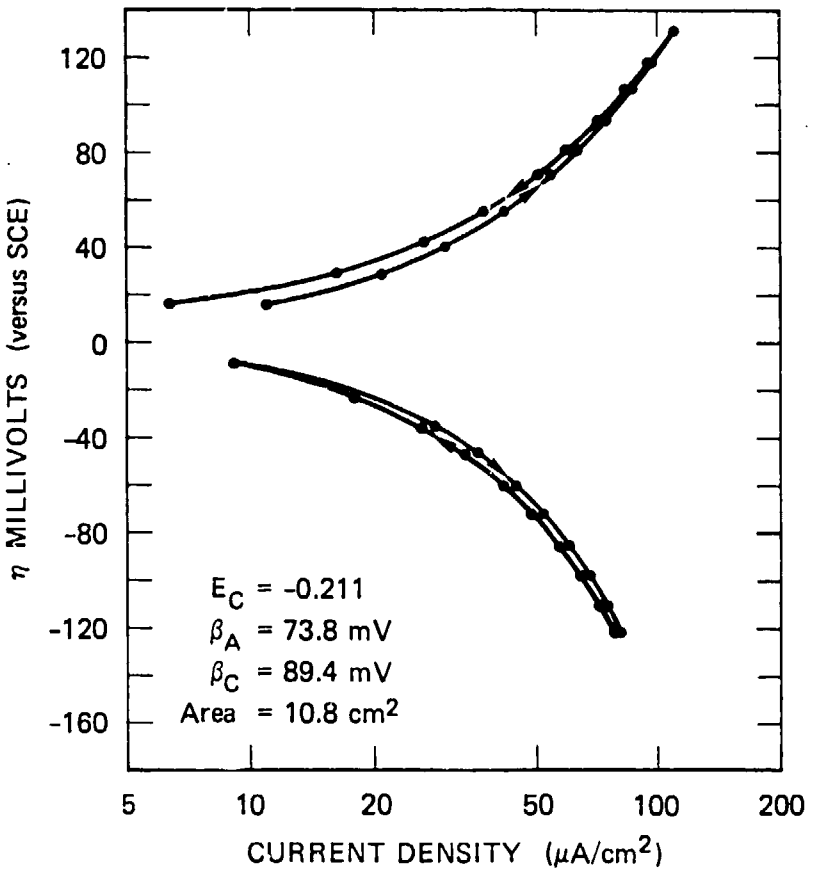

FIGURE 4 TAFEL PLOT FOR A 90/10 COPPER/NICKEL ALLOY EXPOSED TO DEAERATED SULFIDE-POLLUTED SEAWATER FOR 4 DAYS, THEN EXPOSED TO AERATED UNPOLLUTED SEAWATER FOR 4 HOURS

This plot is typical of all exposure histories and environments used in this investigation.

Figure 5 illustrates the effect of environment, exposure time, and exposure history on the corrosion rates of the 90/10 Cu/Ni specimens. These data confirm the work of Syrett et al.[13-20] In particular, these data show that the corrosion rate of specimens exposed to DS-seawater, Figure 5(a) is lower than the rate for samples exposed to A-seawater, Figure 5(b). The initial corrosion rates differ by a factor of six. This indicates that the 800 mpy attack of Cu/Ni alloys cannot be explained by exposure to deaerated, sulfide-polluted seawater alone.

Figure 5 also indicates that 90/10 Cu/Ni samples preexposed to DS-seawater, Figure 5(a), and then exposed to A-seawater, Figure 5(b), corroded faster than samples not preexposed to sulfide. The initial corrosion rates of samples preexposed to DS-seawater and then exposed to A-seawater was about 1.4 times as fast as "fresh" samples that were not preexposed to sulfide. Although the corrosion rate of the preexposed sample dropped below the corrosion rate of the fresh sample after about 12 hours of exposure to A-seawater, the converse was true after four days of exposure and the corrosion rate of the preexposed sample remained higher for about ten days.

The high initial corrosion rate and the higher corrosion rates during the last 10 days of the exposure to A-seawater caused the total weight loss to be greater for the sulfide-preexposed samples. The difference in weight loss between a sulfide-preexposed sample and a fresh sample exposed to the A-seawater was less than 20%. Although the difference in weight loss is small and the errors potentially large, these results agree well with previous experiments.[13] Thus, even though it takes longer for the sulfide preexposed samples to passivate in aerated unpolluted seawater, as compared with fresh samples, the increase in corrosion is still not great enough to be responsible for the accelerated attack of Cu/Ni alloys.

The most dramatic increase in corrosion rate was noted when the Cu/Ni alloys are exposed to AS-seawater, Figure 5(c). The maximum corrosion rate under these conditions was 240 $\mu g\ m^{-2}s^{-1}$ ($\sim$ 33 mpy). This should be compared with the corrosion rate of 0.60 $\mu g\ m^{-2}s^{-1}$ (0.083 mpy) measured on samples exposed to A-seawater for 16 days. Thus, corrosion rate of

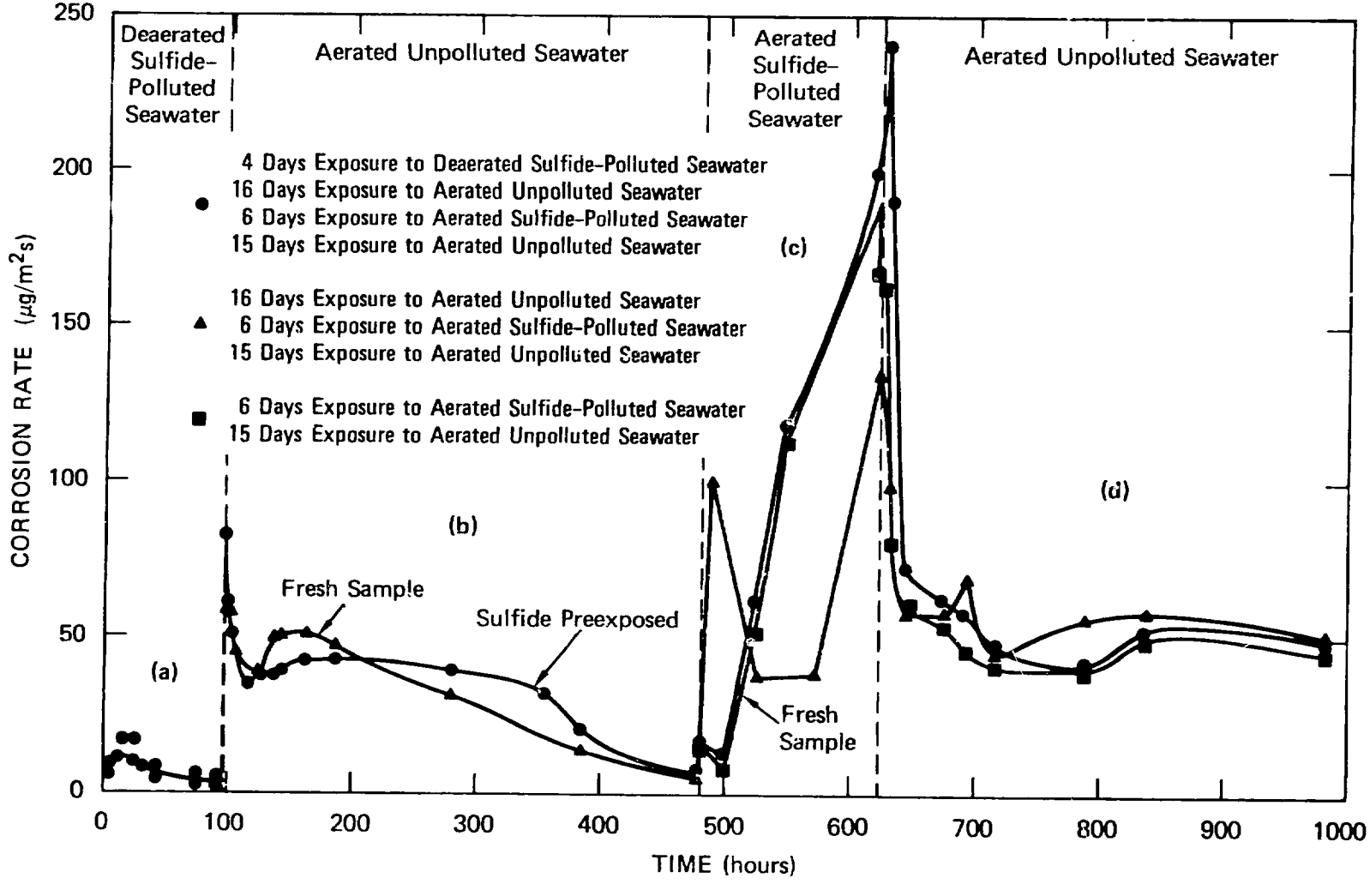

FIGURE 5 CORROSION RATES FOR 90/10 COPPER/NICKEL ALLOY IN FLOWING SEAWATER, SHOWING THE EFFECT OF EXPOSURE HISTORY AND SEAWATER CHEMISTRY

(pH = 8.1 ± 0.2, Temperature = 23.2 ± 1.3°C, Reynolds Number ≅ 44,000, Area = 10.8 cm^2)

of Cu/Ni alloys in AS-seawater is up to 400 times greater than long-term corrosion rates in A-seawater. This dramatic increase in corrosion rate caused by simultaneous exposure to sulfide and oxygen seems to account for the accelerated attack of Cu/Ni alloys in seawater observed by the Navy and the public utilities.

It should be emphasized that these corrosion rates are based on the assumption that the total exposed surface of the specimen corrodes uniformly. If the presence of sulfide results in the formation of localized attack, the local corrosion rates could be much higher than those reported in Figure 5(c). The corrosion rates in this environment also seem to increase with exposure time.

The AS-seawater data, Figure 5(c) show some indication that samples preexposed to A-seawater corrode more slowly than fresh samples and more slowly than samples first preexposed to DS-seawater, than to A-seawater. This seems to indicate that a sulfide-free corrosion product will offer some protection against the accelerated attack. However, even this protective oxide film cannot keep the corrosion rate low for longer than three days in AS-seawater. After three days, the corrosion rate of the "passivated" sample (preexposed only to A-seawater) increased rapidly. In addition, a sulfide-containing corrosion film offers little or no protection and may even accelerate the corrosion in the AS-seawater. These results support those of Gudas and Hack,[1] who showed that preexposure to aerated, unpolluted seawater for several months did impart corrosion resistance to Cu/Ni alloys in aerated, sulfide-polluted environments.

The specimens preexposed to AS-seawater repassivate more slowly in the A-seawater, Figure 5(d), than fresh samples or samples preexposed to DS-seawater. The corrosion rate of specimens preexposed to AS-seawater is more than ten times greater than that of fresh samples after 15 days exposure to A-seawater.

Surface Examination of Corrosion Films

To facilitate the determination of the corrosion mechanism of Cu/Ni alloys in sulfide-polluted seawater, we examined several specimens representing different environmental exposure histories by scanning electron microscopy (SEM).

Energy dispersive X-ray analysis (EDX) was used to characterize the film composition. To facilitate comparisons, the K_α peak heights for each corrosion product were measured using a constant copper K_α peak height.

The structure of the corrosion product developed on a 90/10 Cu/Ni alloy during a 10-day exposure to A-seawater is shown in Figure 6. The corrosion film is composed of two parts: a thick porous layer of corrosion product covering the entire surface (Figure 6a) and a thin, compact layer beneath the thick outer layer (Figure 6b).

The composition of the corrosion film formed on 90/10 Cu/Ni alloys both in synthetic and natural aerated unpolluted seawater has been reported previously.[7,20] These studies indicated that the thick, outer layer of the corrosion film is composed of porous $Cu_2(OH)_3Cl$, and the thin, inner layer is composed of Cu_2O doped with Cl and Ni. (Note that the adherence of the $Cu_2(OH)_3Cl$ is low, so much of it detaches from the metal surface under flowing conditions.) Furthermore, the iron and nickel content was observed to be higher in the outer layer than in the inner layer. Our compositional analyses of the corrosion film formed after a 10-day exposure to unpolluted, aerated seawater agree with these previous results.

The structure and composition of the corrosion product developed on 90/10 Cu/Ni alloys exposed for four days to DS-seawater is shown in Figure 7. This corrorsion film can also be divided into an inner and an outer layer. The outer layer, Figure 7(a), is again rather thick and porous relative to the inner layer. The inner layer, Figure 7(b) shows trenches or ditches along the grain and twin boundaries and is cracked in places. The accompanying EDX measurements, Figure 7(c) and (d). show that the outer layer is high in S but low in Ni and Fe relative to the inner layer.

Figure 8 shows the sulfur, nickel, copper, and oxygen profiles through the thin inner layer, as obtained by Auger analysis. These results support previous studies,[13,14] which indicated that the outer layer is composed primarily of Cu_2S and that the thin inner corrosion product layer is composed primarily of Cu_2O doped with sulfur.

(a) OUTER CORROSION LAYER

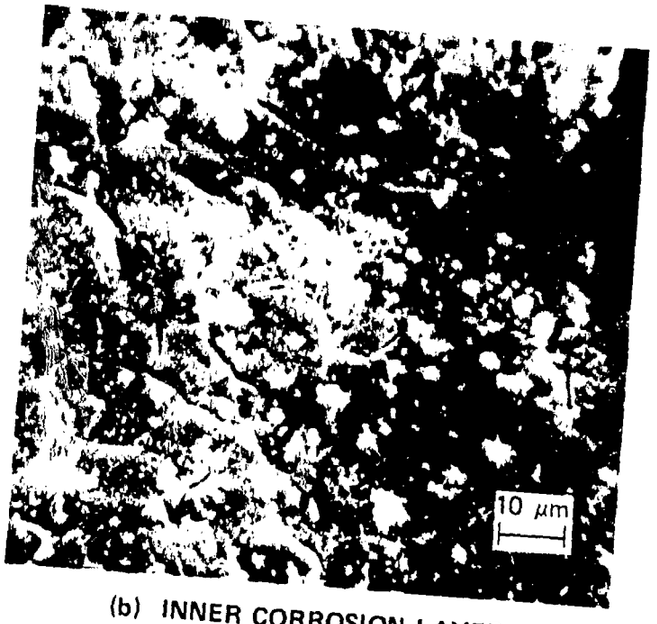

(b) INNER CORROSION LAYER

MP-6077-114

FIGURE 6 SCANNING ELECTRON MICROSCOPY OF CORROSION FILM STRUCTURE ON A 90/10 COPPER/NICKEL ALLOY EXPOSED TO UNPOLLUTED AERATED SEAWATER FOR 10 DAYS

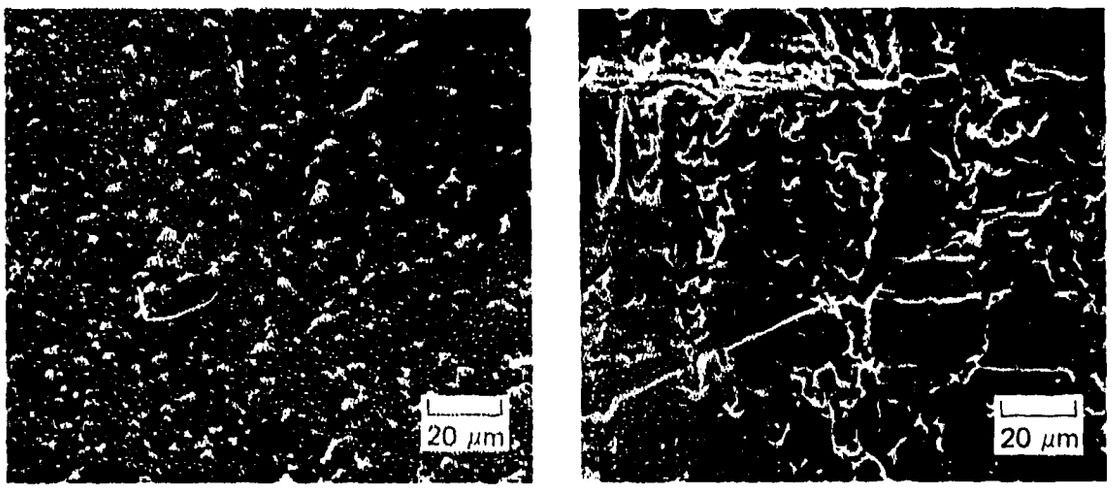

(a) OUTER CORROSION LAYER (b) INNER CORROSION LAYER

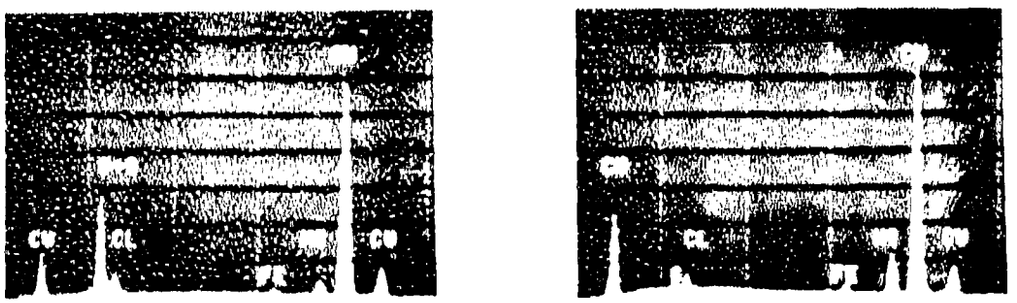

(c) OUTER CORROSION LAYER (d) INNER CORROSION LAYER

MP-6077-115

FIGURE 7 STRUCTURE AND COMPOSITION OF THE CORROSION FILM DEVELOPED ON A 90/10 COPPER/NICKEL ALLOY EXPOSED TO DEAERATED SULFIDE-POLLUTED SEAWATER FOR 4 DAYS

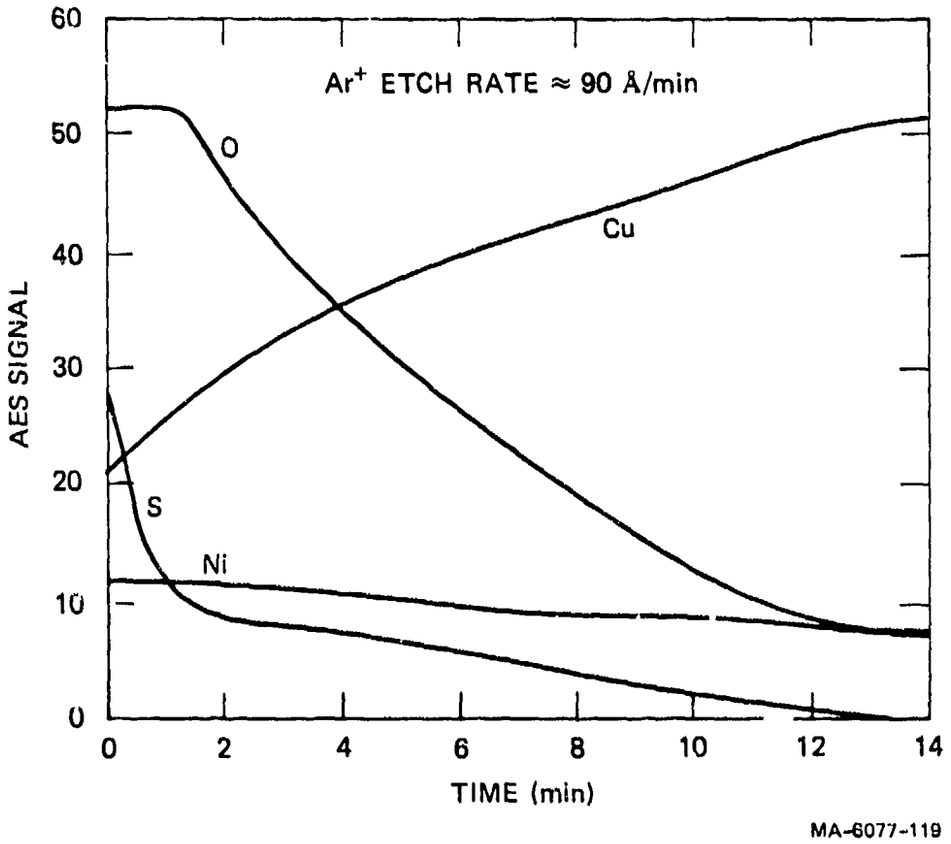

FIGURE 8 AUGER ANALYSIS OF INNER SUBSCALE ON 90/10 COPPER/NICKEL ALLOY EXPOSED TO DEAERATED SULFIDE-POLLUTED SEAWATER ($[S^{=}] = 0.85\ g/m^3$)

Figure 9 shows the structure and composition of corrosion films developed on 90/10 Cu/Ni alloys that had been exposed alternatively to polluted, then unpolluted, seawater. The exposure cycle was as follows: first the specimen was exposed for 4 days to DS-seawater, then exposed for 16 days to A-seawater, then exposed for 6 days to AS-seawater, and finally exposed to A-seawater for 15 days. As shown in Figure 9, the corrosion product developed on this specimen can also be divided into an inner and an outer layer. The outer layer is lower in Ni and Fe and higher in Cl content than the base metal. The inner layer was higher in Ni and Fe content than the base metal. This element distribution in the corrosion film is consistent with the supposition that the outer layer is composed of $Cu_2(OH)_3Cl$ and Cu_2S particles and that the inner layer is Cu_2O doped with S and Cl. Again, the outer layer is porous and thick, while the inner layer shows grain and twin boundary ditches with occasional cracking.

The structure and composition of the corrosion product developed on a specimen* of 90/10 Cu/Ni alloy exposed for 5 weeks in flowing, untreated James River water was also examined. The water was known to have been polluted with sulfide during the exposure period. The structure, shown in Figure 10, was similar to that developed on specimens alternatively exposed to polluted and unpolluted seawater in our test loop. The corrosion product could again be divided into a thick, porous outer layer and a thin, cracked inner layer. As shown in Figure 11, the outer layer was high in Ni, Fe, Cl, and S content relative to both the inner layer and the base metal. These elemental distributions are consistent with the suggestion that the outer layer is composed of porous Cu_2S and $Cu_2(OH)_3Cl$ doped with Ni, Fe, and S, while the inner layer is most likely composed of Cu_2O doped with S and Cl. Therefore, the corrosion product developed on the James River specimens was very similar to the corrosion product developed on samples exposed to AS-seawater in our test loop.

*Specimen provided through the courtesy of H. Hack, David W. Taylor Naval Ship Research and Development Center, Annapolis, MD.

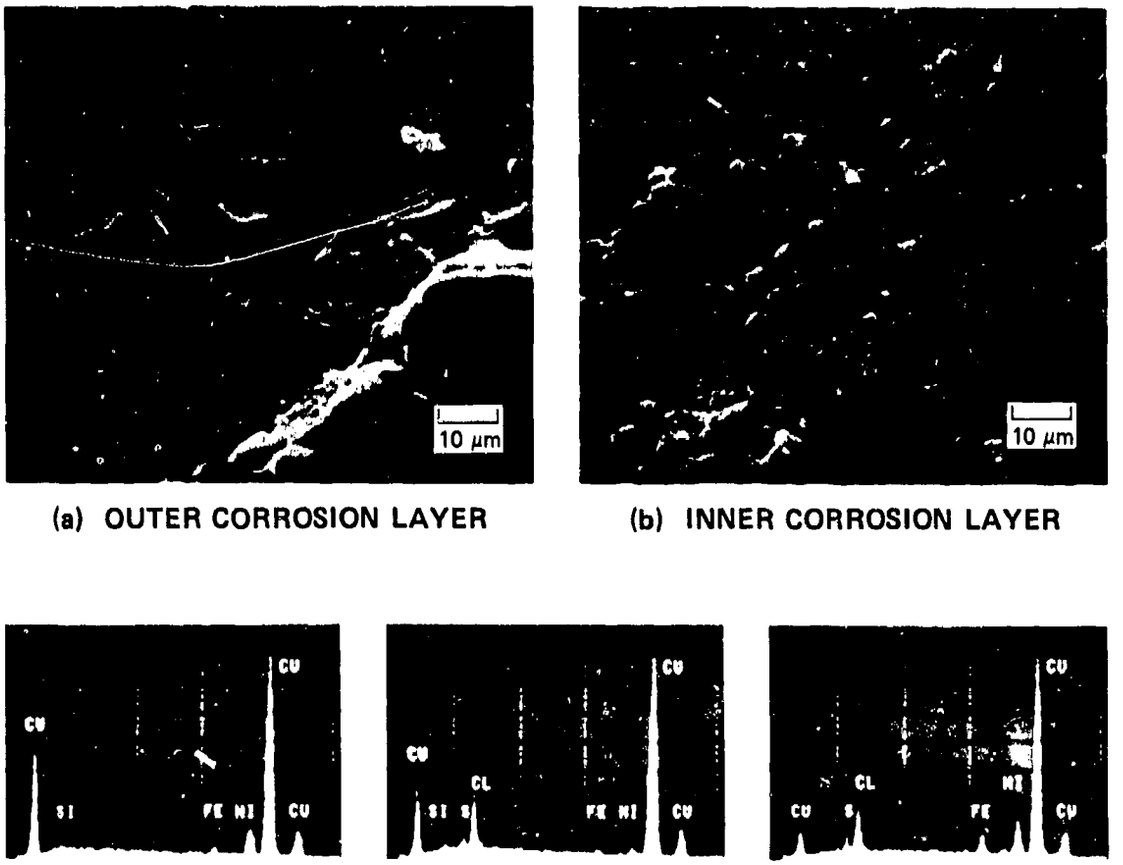

(a) OUTER CORROSION LAYER

(b) INNER CORROSION LAYER

(c) BASE METAL

(d) OUTER CORROSION LAYER

(e) INNER CORROSION LAYER

MP-6077-116

FIGURE 9 STRUCTURE AND COMPOSITION OF THE CORROSION FILM DEVELOPED ON A 90/10 COPPER/NICKEL ALLOY EXPOSED TO DEAERATED SULFIDE-POLLUTED SEAWATER FOR 4 DAYS, AERATED UNPOLLUTED SEAWATER FOR 16 DAYS, AERATED SULFIDE-POLLUTED SEAWATER FOR 6 DAYS, AND AERATED UNPOLLUTED SEAWATER FOR 15 DAYS

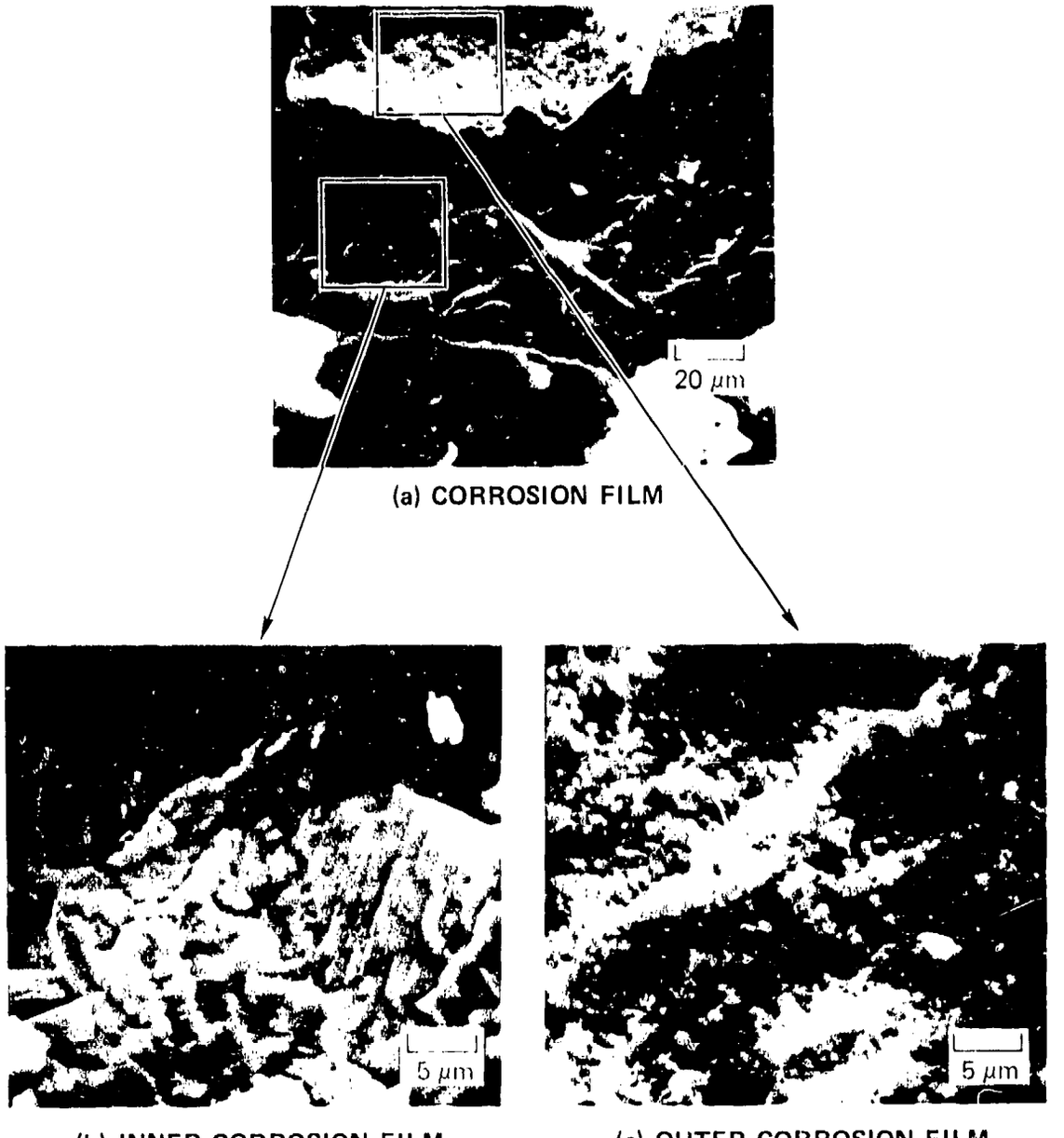

FIGURE 10 SCANNING ELECTRON MICROSCOPY OF THE CORROSION FILM DEVELOPED ON A 90/10 COPPER/NICKEL ALLOY TAKEN FROM THE UPSTREAM PIPE SECTION OF THE JAMES RIVER TEST LOOP

The specimen was exposed to untreated James River water for 5 weeks. Flow was not turbulent at this section of pipe.

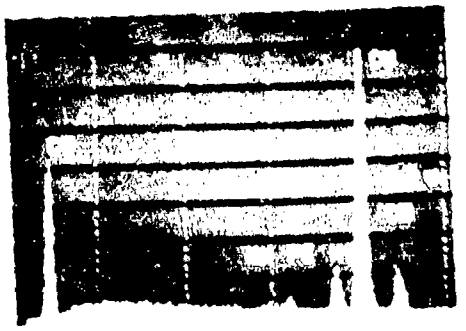

(a) ANALYSIS OF THE BASE METAL

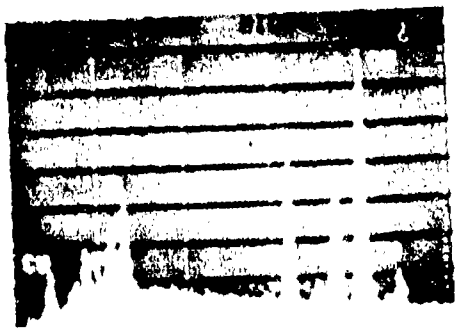

(b) ANALYSIS OF OUTER CORROSION FILM SURFACE

(c) ANALYSIS OF INNER CORROSION FILM SURFACE

MP-6077-118

FIGURE 11 COMPOSITION OF CORROSION FILM DEVELOPED ON THE SPECIMEN SHOWN IN FIGURE 10

IV DISCUSSION

Effect of Dissolved Oxygen Content on the Corrosion Behavior of Cu/Ni Alloys in Unpolluted Seawater

The mechanism of corrosion in unpolluted seawater environments needs to be established in order to understand the process of accelerated attack of Cu/Ni alloys in a sulfide-polluted seawater environment. Since the effect of dissolved oxygen concentration in the seawater on the corrosion rates and corrosion potential of Cu/Ni alloys provides some of the information needed to understand the mechanism of corrosion of these alloys in unpolluted seawater we present here a model for that effect.

Figure 12 illustrates the experimentally observed[18,20] effect of dissolved oxygen content on the corrosion potential of a 90/10 and a 70/30 Cu/Ni alloy after exposure to seawater for 200 hours. Corrosion potentials obtained in nominally deaerated seawater ($\leq$ 0.045 g/m^3 oxygen) have been included in Figure 12. However, it must be emphasized that, at such low oxygen concentrations, the exchange current density for the oxygen reaction is quite low; thus, the corrosion potentials become quite low; thus, the corrosion potentials become quite sensitive to unknown and unpredictable redox reactions that have exchange currents of the same order as the oxygen reaction. In other words, corrosion potentials are much less dependent on the oxygen concentration in this range. Also, at dissolved oxygen concentrations up to $\sim$ 26 g/m^3 in the seawater, the corrosion potential of the 90/10 Cu/Ni alloy is consistently higher than the corrosion potential of the 70/30 alloy in aerated, unpolluted seawater. Furthermore, both alloys show an increase in corrosion potential with increasing oxygen concentration in this higher range of oxygen concentrations (0.85-26.3 g/m^3). The corrosion potential increased slightly (90/10 Cu/Ni) or significantly (70/30 Cu/Ni) on decreasing the oxygen content from 0.85 g/m^3 to $\leq$ 0.045 g/m^3.

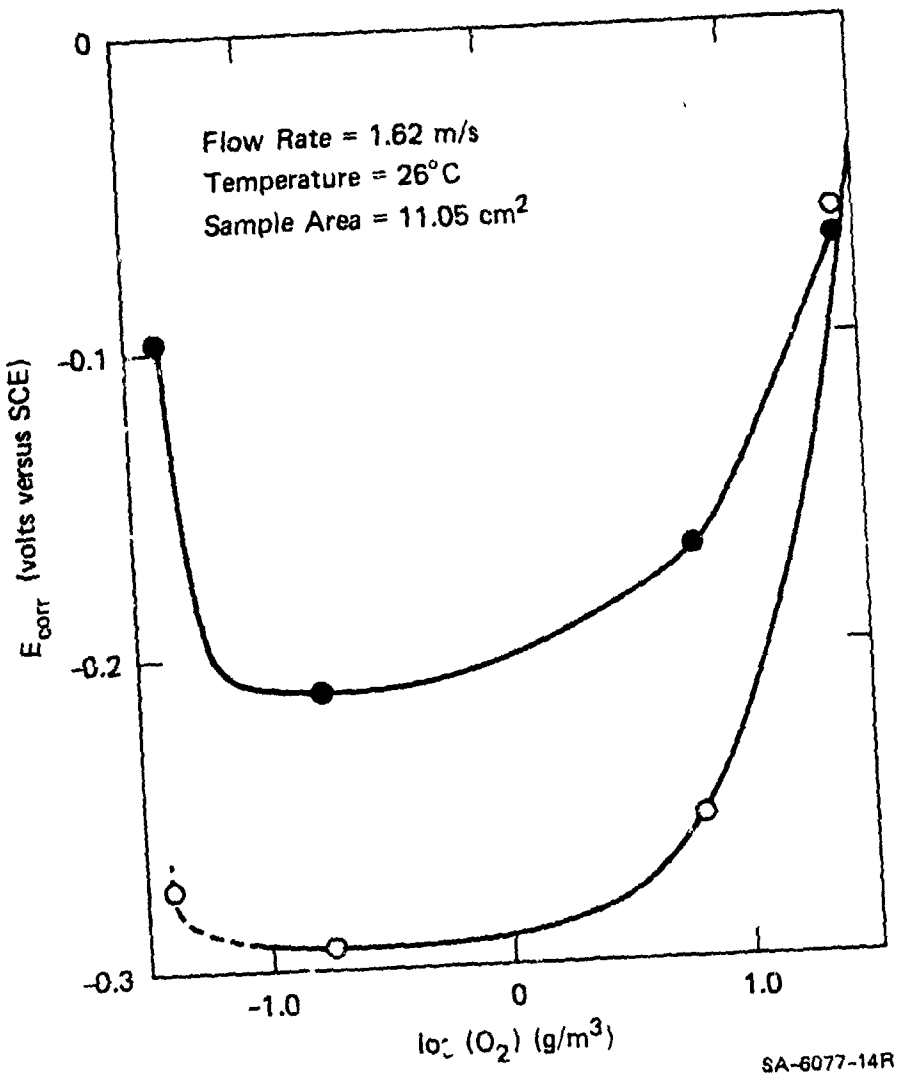

FIGURE 12 VARIATION OF THE CORROSION POTENTIAL (E_{corr}) WITH OXYGEN CONCENTRATION (g/m^3) FOR 90/10 Cu/Ni ALLOY (O) AND 70/30 Cu/Ni ALLOY (●) AFTER 200 HOURS EXPOSURE TO FLOWING SEAWATER

Figure 13 shows the experimentally observed[18,20] effect of dissolved oxygen in unpolluted seawater on the $1/R_p$* values on the two Cu/Ni alloys. Except at very high dissolved oxygen concentrations ($\sim$ 26 g/m^3), the corrosion rate of the 90/10 Cu/Ni alloy is higher than the corrosion rate of the 70/30 Cu/Ni alloy. The corrosion rate of 90/10 Cu/Ni alloy decrease with increasing oxygen concentration, at least up to 6.6 g/m^3 oxygen (air-saturated).

It is possible that the corrosion rate after a 200-hr exposure increases slightly on increasing the oxygen content from 6.6 g/m^3 to 26.3 g/m^3, but this was not so for shorter exposures[20]: after 20, 50, or 100 hr in seawater, the corrosion rate of 90/10 Cu/Ni alloy decreases continuously with increasing oxygen content. The corrosion rate of 70/30 Cu/Ni alloy, on the other hand, showed a very definite increase upon increasing the oxygen content from 6.6 g/m^3 to 26.3 g/m^3 for exposure periods greater than 50 hr; at oxygen concentrations below 6.6 g/m^3, the 70/30 Cu/Ni alloy behaved like the 90/10 Cu/Ni alloy in that corrosion rates increased as oxygen content decreased for exposure times of at least 200 hr.

As indicated previously, it is not entirely clear why the corrosion potentials of the Cu/Ni alloys (particularly the 70/30 Cu/Ni alloy) tend to shift toward more noble values as the oxygen concentration is reduced from 0.85 g/m^3 to $\leq$ 0.045 g/m^3. This aside, effects of dissolved oxygen on the corrosion behavior of Cu/Ni alloys can be explained by means of the two Evans diagrams shown in Figure 14. Figure 14(a) illustrates the corrosion behavior at low to medium dissolved oxygen concentrations (up to $\sim$ 7 g/m^3). At these oxygen levels, the corrosion rate responds to an incremental increase in dissolved oxygen by forming a more protective corrosion product film over the alloy in a given exposure time. This protective layer then separates the corrosion product seawater

*R_p is the polarization resistance, which, as shown in the Appendix, is inversely proportional to the corrosion rate.

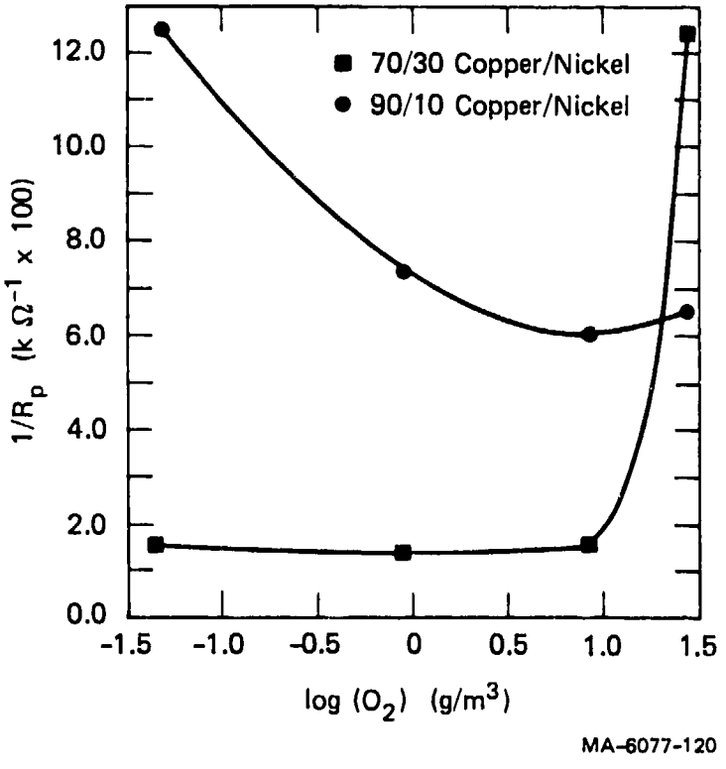

FIGURE 13 RECIPROCAL POLARIZATION RESISTANCE ($1/R_p$) OF COPPER/NICKEL ALLOYS EXPOSED TO UNPOLLUTED AERATED SEAWATER FOR 200 HOURS AT A FLOW RATE OF 1.62 m/s AS A FUNCTION OF OXYGEN CONCENTRATION

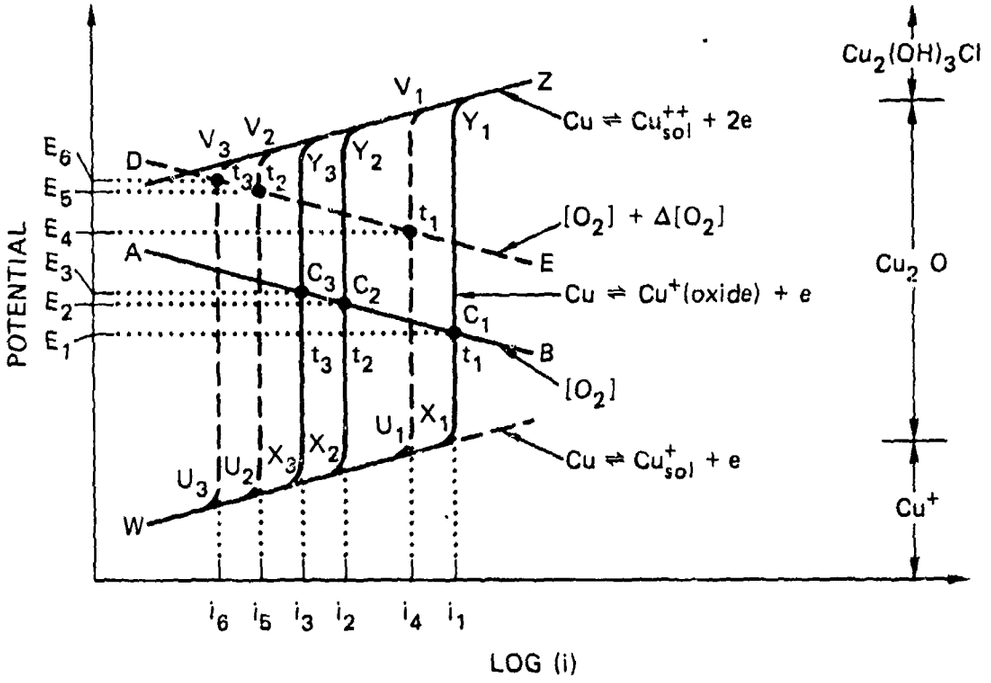

(a) 0.045 < OXYGEN < 7 ppm

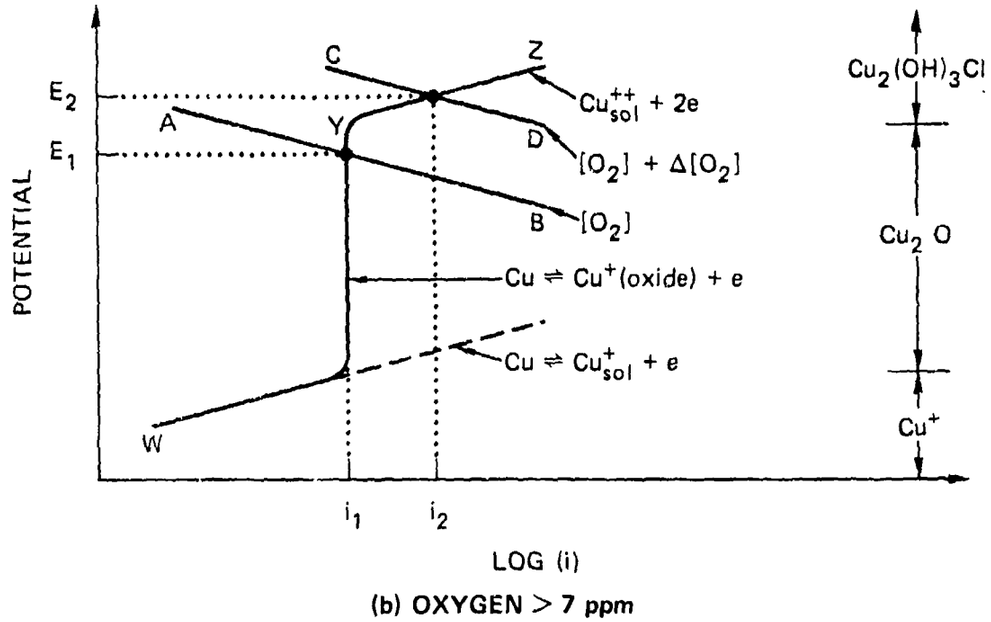

(b) OXYGEN > 7 ppm

MA-6077-122

FIGURE 14 EFFECT OF OXYGEN CONCENTRATION ON CORROSION CURRENTS OF COPPER/NICKEL ALLOYS IN AERATED UNPOLLUTED SEAWATER

interface (cathode) from the metal/corrosion product interface (anode). The process can be represented by:

$$\text{cathode} \quad O^{ads} + 2Cu^{Cu_2O} \rightleftharpoons 2V^{Cu_2O} + 2p^{Cu_2O} + O^{Cu_2O} \qquad (1)$$

$$\text{anode} \quad 2Cu^{M} + 2V^{Cu_2O} + 2p^{Cu_2O} \rightleftharpoons 2V^{M} + 2Cu^{Cu_2O} \qquad (2)$$

where:

O^{ads} = oxygen adsorbed on the Cu_2O surface

Cu^{Cu_2O} = cation in Cu_2O

V^{Cu_2O} = cation vacancy in Cu_2O

p^{Cu_2O} = electron hole in Cu_2O

O^{Cu_2O} = anion in Cu_2O

Cu^{M} = Cu in base metal

V^{M} = Cu vacancy in base metal.

The surface corrosion product is most likely Cu_2O. It is a p-type semiconductor, and an IR drop develops across the oxide between the anodic and cathodic reaction sites.

Consider first an oxygen concentration that yields the cathodic reduction curve AB in Figure 14(a). At time t_1, the metal oxidation reaction is represented by curve WX_1Y_1Z, and the corrosion current and corrosion potential are i_1 and E_1, respectively. While the measured corrosion potential is E_1, the potential at the metal/metal oxide interface is more active than this value by an amount equal to the IR drop (i.e., C_1X_1 in Figure 14a). After an exposure time t_2 ($> t_1$), the oxide film grows, the IR drop increases, and the metal oxidation reaction is now represented by curve WX_2Y_2Z. This results in a decrease in corrosion current to i_2 and an increase in corrosion potential to E_2. Similarly, at time t_3, the corrosion potential will have increased to E_3 and the corrosion current will have decreased to i_3.

Next, suppose a fresh sample is exposed and the dissolved oxygen content is increased by an amount of ΔO_2. The cathodic redox potential

shifts to higher (more noble) values yielding curve DE in Figure 14(a). After the same exposure time of t_1, the metal oxidation reaction is represented by the broken curve WU_1V_1Z. At this new, higher oxygen content, the IR drop is higher than it was at the original lower oxygen concentration because the corrosion film growth is much higher at the higher oxygen concentration. This increase in the IR drop is more than enough to compensate for the noble shift in the cathodic process. Therefore, the overall effect of an incremental increase in the dissolved oxygen concentration is to decrease the corrosion current and increase corrosion potential to i_4 and E_4, respectively.

After an exposure time of t_2, the corrosion film grows even thicker, resulting in an even larger IR drop and corresponding decrease in the corrosion potential and corrosion rate to E_5 and i_5, respectively. The corrosion behavior shown in Figures 12 and 13 (for oxygen concentrations up to $\sim$ 7 g/m^3) is therefore explained by the increase in film growth with an incremental increase in oxygen concentration.

Additionally, the effect of time on the corrosion rate (Figure 5b) is explained by the general increase in film thickness (therefore IR drop) with increasing time, irrespective of the oxygen concentration. This increase in IR drop is responsible for the observed increase in corrosion potential and decrease in corrosion rate with an increase in exposure time. Note also that the effect of additional exposure time t_3 has less of an effect on the corrosion rate because the Cu_2O growth probably follows a parabolic rate law.[29]

The corrosion behavior at high oxygen concentrations (> 7.0 g/m^3) is different from that observed at the lower oxygen concentrations. The effect of both exposure time and an incremental increase in oxygen concentration on the corrosion behavior is modified. At high oxygen concentrations, the metal starts to corrode at much faster rates than at the lower oxygen concentrations. This corrosion process can be modeled as an electrochemical process in which the anodic reaction forms soluble Cu^{++} ions or perhaps $Cu_2(OH)_3Cl$. The cathodic process is oxygen reduction, and at these high oxygen concentrations, the corrosion potential is high

enough to make Cu^{++}_{sol} the stable corrosion species instead of the protective Cu_2O formed at lower oxygen concentrations. The film dissolution process can be represented as:

$$\text{anode} \quad 2Cu^{Cu_2O} \rightleftharpoons 2Cu^{++}_{sol} + 2e^{Cu_2O} + 2V^{Cu_2O}_{Cu} \tag{3a}$$

$$\text{or} \quad 2Cu^{M} \rightleftharpoons 2Cu^{++}_{sol} + 2e^{M} + 2V^{M} \tag{3b}$$

$$\text{cathode} \quad 2e^{Cu_2O} + 1/2(O_2) + H_2O \rightleftharpoons 2(OH)^- \tag{4}$$

where Cu^{++}_{sol} = copper cations in solution. These reactions take place at the corrosion film/solution interface. In addition, the chemical precipitation reaction

$$2(Cu^{++}_{sol}) + 3(OH)^- + Cl^- \rightleftharpoons Cu_2(OH)_3Cl \tag{5}$$

occurs and results in the formation of only a nonprotective layer covering the metal. The corrosion process described by equations (3) and (4) therefore results in high corrosion rates because a protective oxide layer is not formed, equation (3b), or as shown in equation (3a), the protective Cu_2O is dissolved.

Figure 14(b) illustrates our model for this behavior. Note that, for an incremental increase in oxygen concentration, $\Delta[O_2]$, the cathodic redox potential shifts to more noble values. The corresponding corrosion rates and corrosion potentials increase from i_1 and E_1 to i_2 and E_2, respectively, with this incremental increase in $[O_2]$.

The lower oxygen reduction curve AB intersects the metal oxidation curve WXYZ in the passive range of potentials where the protective Cu_2O is the stable phase. This situation arise, for instance, for 70/30 Cu/Ni in seawater containing $\lesssim 6.6$ g/m^3 oxygen for exposure periods of up to 200 hr.

The higher oxygen reduction curve CD, on the other hand, intersects the metal oxidation curve in the potential range in which the nonprotective $Cu_2(OH)_3Cl$ is stable. This situation arise, for instance, for 70/30 Cu/Ni in seawater containing 26.3 g/m^3 oxygen for exposure times exceeding about 50 hr.[20]

The transition from a corrosion product that is primarily Cu_2O (protective) to one that is primarily $Cu_2(OH)_3Cl$ (nonprotective) explains how the corrosion rate of 70/30 Cu/Ni alloy increase dramatically upon increasing the oxygen content from 6.6 g/m^3 to 26.3 g/m^3. Futhermore, since the IR drop through a $Cu_2(OH)_3Cl$ surface film is negligible compared with that through Cu_2O, it is clear that the corrosion rate of 70/30 Cu/Ni in the high oxygen environment will not decrease appreciably with time of exposure, as observed.[20]

It is important to realize that the transition from a Cu_2O corrosion product to $Cu_2(OH)_3Cl$ is not normally abrupt, but occurs gradually over a range of potentials. The intersection of curves CD and WXYZ, Figure 14(b), in the $Cu_2(OH)_3Cl$ zone does not mean that Cu_2O is necessarily absent; rather that $Cu_2(OH)_3Cl$ will predominate. Furthermore, the time-dependent series of metal oxidation curves shown in Figure 14(a) (WX_1Y_1Z, WX_2Y_2Z, WX_3Y_3Z) illustrates how such a transition from Cu_2O to $Cu_2(OH)_3Cl$ occurs with increasing time of exposure. Thus, an increase in oxygen concentration from 6.6 g/m^3 to 26.3 g/m^3 caused a decrease in the corrosion rate of 90/10 Cu/Ni alloy (as illustrated in Figure 14a) for exposure periods of up to 100 hr, [20] but a slight increase in the corrosion rate after a 200-hr exposure (Figure 13). This observation suggests that, after 100 hr in the high oxygen environment, the corrosion potential was still in the passive range (Cu_2O zone), but that after 200 hr the corrosion potential had increased sufficiently that a substantial quantity of nonprotective $Cu_2(OH)_3Cl$ was being produced.

The increase in corrosion potential (Figure 12) and decrease in corrosion rate (Figure 13) with increasing nickel concentration result from the nickel doping the Cu_2O, resulting in a greater IR drop. This increase in IR drop acts to increase the corrosion potential while causing

a decrease in the corresponding corrosion rate. Furthermore, the dependence of the corrosion rate on dissolved oxygen concentration (Figure 13) is much lower for the 70/30 Cu/Ni alloy than for the 90/10 Cu/Ni alloy at oxygen concentrations up to 6.6 g/m^3. The effect of nickel alloying on the slopes of these curves is most likely explained by the nickel acting to decrease the time required to establish a steady state oxide thickness. Thus, after 200 hr, the oxide thickness and IR drop are essentially independent of oxygen concentration for 70/30 Cu/Ni, whereas the oxide on 90/10 Cu/Ni is still thickening after 200 hr at all oxygen concentrations. During the period that the oxide is still growing on the 70/30 Cu/Ni, say, up to 100 hr of exposure, its corrosion rate is actually somewhat more dependent on oxygen concentration than the corrosion rate of the 90/10 Cu/Ni.[20]

The increase in IR drop with the addition of Ni, Fe, and Cl (hence the decrease in film conductivity) can be explained by assuming that the corrosion product, composed mainly of Cu_2O, is a p-type semiconductor doped with the Ni, Fe, and Cl.

$$4p^{Cu_2O} + 2Ni^{M} + 2V^{Cu_2O} \rightleftharpoons 2Ni^{Cu_2O} + 2V^{M} \quad (6)$$

$$6p^{Cu_2O} + 2Fe^{M} + 2V^{Cu_2O} \rightleftharpoons 2Fe^{Cu_2O} + 2V^{M} \quad (7)$$

$$Cl^{ads} + 2Cu^{Cu_2O} \rightleftharpoons Cl^{Cu_2O} + 2V^{Cu_2O} + p^{M} \quad (8)$$

where

Fe^{M}, Ni^{M} = iron or nickel site in Cu/Ni base metal

Fe^{Cu_2O}, Ni^{Cu_2O} = iron or nickel at cation site in Cu_2O

Cl^{ads} = chlorine absorbed at Cu_2O/seawater interface

Cl^{Cu_2C} = chlorine at anion site in Cu_2O.

Nickel and iron act as electron donors to the Cu_2O layer and therefore reduce its conductivity since it is a p-type semiconductor. The replacement

of oxygen reduction, equation (1) with chlorine reduction, equation (8) also results in a decrease in conductivity since equation (8) generates one hole, whereas equation (1) generates two holes.

In summary, the corrosion behavior of Cu/Ni alloys in unpolluted seawater is controlled by the protective inner oxide film. This oxide film is most likely composed of Cu_2O doped with Cl, Ni, and Fe as described in the surface examination of corrosion films (Section III) and by Kato et al.[7] The effect of alloying with nickel and iron is to slow the rate of transport of metal ions through the oxide by decreasing the oxide conductivity.[3,30-33] The film growth rate controls the IR drop across the film by separating the anodic reaction at the metal oxide interface from the cathodic reaction at the oxide/seawater interface. Additionally, after relatively short exposure periods at high oxygen concentrations (e.g., 26.3 g/m^3), the anodic and cathodic reactions, equations (3) and (4) are both located at the seawater interface; hence they are much less affected by an IR drop.

Corrosion Behavior of Cu/Ni Alloys in DS-Seawater

As discussed previously, the DS-seawater used in this study almost certainly contained a trace of oxygen. Thus, the following discussion will cover both the case of oxygen-free sulfide-polluted seawater and the case of our DS-seawater, which contained a trace of oxygen.

The effect of sulfide on the corrosion of Cu/Ni alloys in deaerated seawater or DS-seawater can best be explained by considering its impact on two processes. First, the sulfide prevents the formation of a protective corrosion product. Second, the sulfide precipitates Cu^+ ions at the corrosion product/seawater interface and substantially lowers the Cu^+ ion concentration in solution. This reduction in Cu^+ ion concentration results in an active shift in the anodic redox potential, as illustrated in Figure 15. The cathodic reaction is then either hydrogen ion reduction alone or, if a trace of oxygen is present, a combination of hydrogen ion and oxygen reduction. At the low oxygen concentrations found in DS-seawater, the oxygen reduction reaction is probably diffusion limited; even so, at

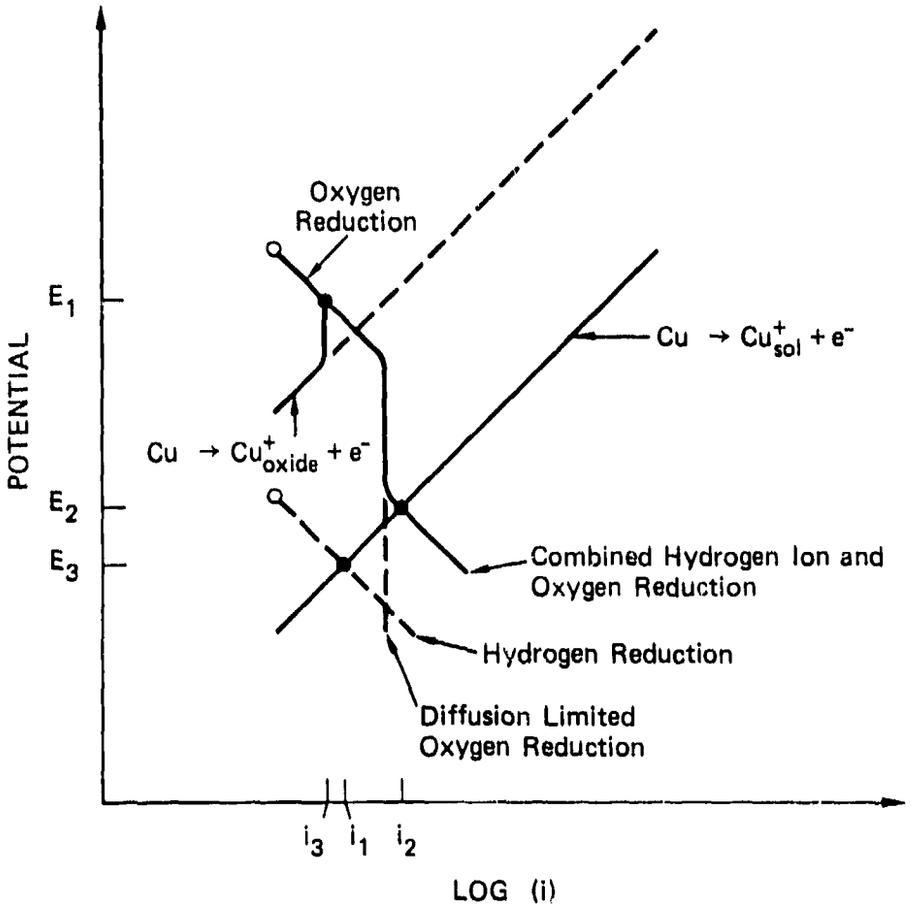

FIGURE 15 EFFECT OF LOW OXYGEN CONTENT SEAWATER WITH AND WITHOUT SULFIDE-POLLUTION ON THE CORROSION CURRENTS OF COPPER/NICKEL ALLOYS

the potentials recorded in DS-seawater [approximately -0.48 V (SCE)], the oxygen reduction reaction would dominate and the cathodic reduction of hydrogen ions would be quite limited, as indicated in Figure 15 for a corrosion potential E_2. In the complete absence of oxygen, only H^+ ions can be cathodically reduced, the potential would drop to E_3, and the corrosion rate would decrease slightly.

The initial anodic reaction product at these potentials is Cu^+ ions, but these react with the dissolved sulfide and precipitate at the metal surface as a nonprotective, porous, black cuprous sulfide scale. The cathodic reaction (reduction of either oxygen or hydrogen ions) occurs at the metal surface beneath the porous cuprous sulfide. The OH^- ions liberated at cathodic sites may react with the anodically produced Cu^+ ions and allow the formation and growth of an oxide-type film beneath the sulfide scale.[9,13] This oxide-type film is primarily cuprous oxide, but it is doped with alloying elements (Ni, Fe) and some of the components of the polluted seawater (S, Si, Cl, Mg, and Ca). The oxide-type film is not protective like the Cu_2O film formed in A-seawater and instead contains cracks and defects. Nevertheless, corrosion rates in sulfide-polluted seawater, with or without a trace of oxygen present, are not particularly high and are of the same order as the corrosion rates in A-seawater after a 200-hr exposure.

Effect of Sulfide Preexposure on the Corrosion Behavior of Cu/Ni in Aerated, Unpolluted Seawater

The effect of sulfide preexposure on the subsequent corrosion behavior of Cu/Ni alloys in aerated seawater is illustrated with the help of Figure 16. At the end of the exposure to DS-seawater (at time t_0), the corrosion potential and corrosion current are E_0 and i_0, respectively. When the DS-seawater is replaced with A-seawater, the cathodic reduction curve shifts to more noble potentials, consistent with the much higher oxygen concentration. In addition, there is a gradual shift from the metal oxidation curve shown in Figure 15 to that shows in Figure 14; the transition is marked by a change from active to passive conditions.

This rather slow change occurs because the environment closest to the metal is initially the DS-seawater contained within the pores of the

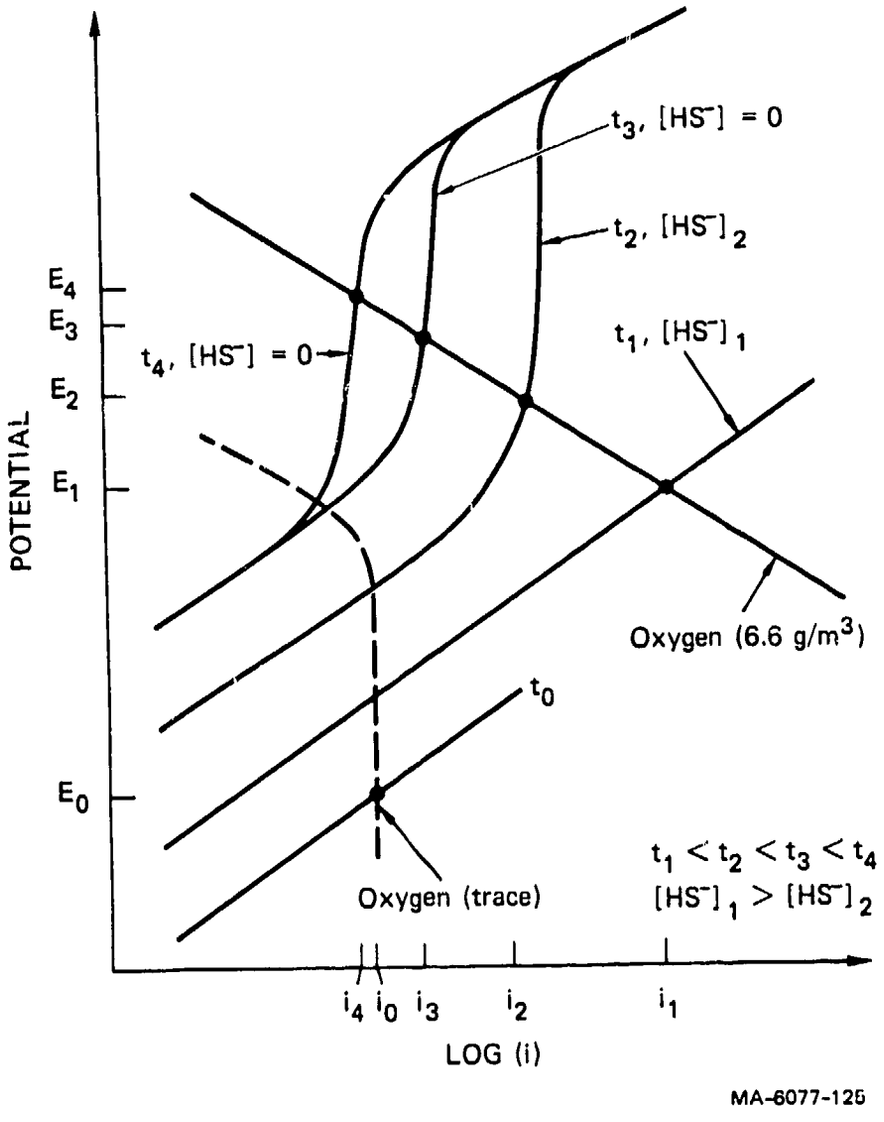

FIGURE 16 EFFECT OF LOW OXYGEN SULFIDE-POLLUTED SEAWATER PREEXPOSURE ON CORROSION CURRENT OF COPPER/NICKEL ALLOYS IN AERATED SEAWATER

sulfide scale. Free sulfide has a half-life of only 17 minutes in aerated seawater,[34] but longer half-lives can be expected in zones of restricted flow (like a porous scale). Furthermore, some of the sulfide oxidation products liberated, like elemental sulfur and polysulfides, behave much the same way as sulfide in their effect on corrosion. Couple this with the possibility that sulfur is also released from the sulfide scale as it transforms slowly to oxide,[13] and it is clear why the environment closest to the metal does not instantly change from DS-seawater to A-seawater.

After a short exposure time, t_1, in the A-seawater, the sulfide content close to the metal is $[HS^-]_1$, so the Cu^+ concentration and therefore the anodic redox potential are still relatively low. This leads to a corrosion potential of E_1 and a high corrosion current, i_1 (Figure 16). At time t_2 ($> t_1$), the sulfide level $[HS^-]_2$ is substantially less, the anodic redox potential has increased, the corrosion potential has increased to E_2, and some passive behavior is seen. At time t_3, essentially all the sulfide has been oxidized to innocuous species so that the condition is like those shown in Figure 14(a): the anodic redox potential has increased to E_3, and the corrosion current has decreased to i_3. At time t_4 and beyond, the behavior is similar to a fresh sample in A-seawater, but for several days following the sulfide preexposure, the corrosion rates of preexposed samples are high compared with those measured on fresh samples.

Corrosion Behavior of Cu/Ni Alloys in AS-Seawater

Figure 5(c) shows that the corrosion rate is considerably higher in aerated, sulfide-polluted seawater than in any other environment. Figure 17 helps to explain this behavior, as follows. In DS-seawater, the corrosion potential is considerably lower and the corrosion current slightly higher than the corrosion potential and corrosion current for deaerated, unpolluted seawater.[14] The active shift in the corrosion potential, as explained previously, is brought about by the large, anodic shift in the anodic redox potential and the anodic shift in the cathodic reaction. The anodic shift in the cathodic reaction, brought about by the limited amount of oxygen available for oxygen reduction, is responsible for keeping the corrosion

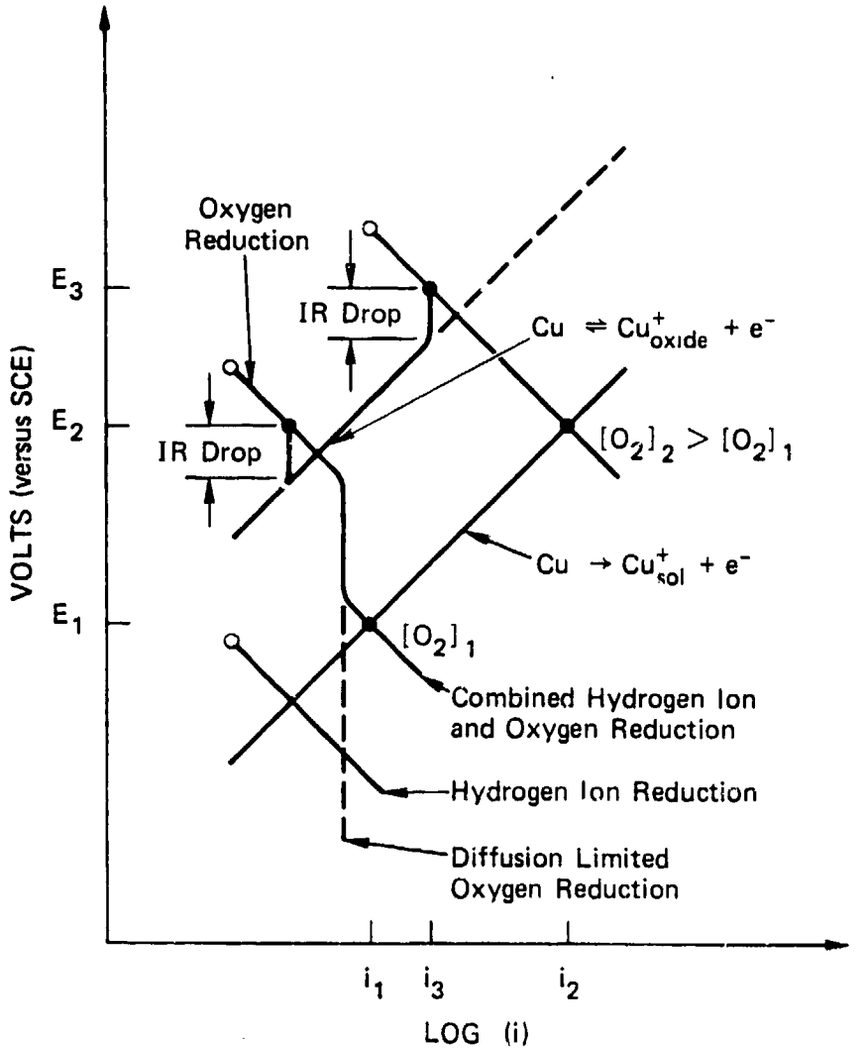

FIGURE 17 EFFECT OF AERATED SULFIDE-POLLUTED SEAWATER ON THE CORROSION CURRENTS OF COPPER/NICKEL ALLOYS

current relatively low in the DS-seawater. Additionally, the sulfide prevents the formation of a protective oxide film, and therefore, the corrosion rate remains relatively constant with increasing exposure time. This is different from the behavior of Cu/Ni alloys in aerated, or de-aerated, unpolluted seawater in which the IR drop of the protective corrosion film becomes important.

If oxygen is introduced into the DS-seawater while continuously supplying sulfide, the cathodic redox potential dramatically increases along with the corrosion rate and the corrosion potential. However, the corrosion potential (E_2 in Figure 17) in this AS-seawater does not exceed -0.25 V (SCE) very often, so the formation of Cu_2O is not favored [Figure 3(b)]. Instead, active corrosion is favored with the production of Cu^+ ions, which subsequently precipitate at the surface as a porous nonprotective sulfide scale. Since the presence of sulfide prevents the formation of a protective corrosion film even in the presence of the higher oxygen concentration, the corrosion rates of Cu/Ni alloys do not decrease with increasing polluted seawater exposure time.

V PROPOSED CORROSION MECHANISMS OF Cu/Ni ALLOYS IN SEAWATER

The corrosion behavior of Cu/Ni alloys in aerated unpolluted seawater is illustrated schematically in Figure 18(a). As suggested by the SEM studies (Section III), the corrosion film that develops is composed of a thick, porous outer layer of $Cu_2(OH)_3$ Cl and a thin, adherent layer of Cu_2O. The outer layer offers little corrosion protection, while the inner layer offers good corrosion protection. During normal corrosion, the cathodic process of oxygen reduction occurs at the interface between the inner and outer corrosion film. The anodic reaction of metal oxidation occurs at the interface between the oxide film and the base metal. The separation of the anode and cathode caused by the intervening oxide film results in an IR drop across this film. This IR drop, which increases with increasing film thickness, controls the Cu/Ni alloy corrosion rate.

While the above process of oxide formation is proceeding, a separate electrochemical process may be occurring simultaneously at the outer/inner corrosion product interface. This process is the dissolution of the oxide. The cathodic process for the oxide dissolution is oxygen reduction, and the anodic process is oxidation of the Cu^+ ions in the Cu_2O film to Cu^{++} ions in solution. These Cu^{++} ions, in turn, are responsible for the formation of the porous outer layer of $Cu_2(OH)_3$ Cl. Therefore, the corrosion behavior of Cu/Ni alloys in unpolluted aerated seawater can be explained by the combined electrochemical process of metal oxidation and Cu_2O dissolution.

When Cu/Ni alloys are exposed to deaerated, sulfide-polluted seawater, a corrosion product develops, as shown in Figure 18(b). Here, again the corrosion film is composed of an inner and an outer corrosion layer. The outer layer is cuprous sulfide, which precipitates as a porous, nonprotective scale by reaction between the anodically produced Cu^+ ions and the dissolved sulfide in the seawater. The inner layer is once again largely cuprous oxide, but it is doped with many other elements, including

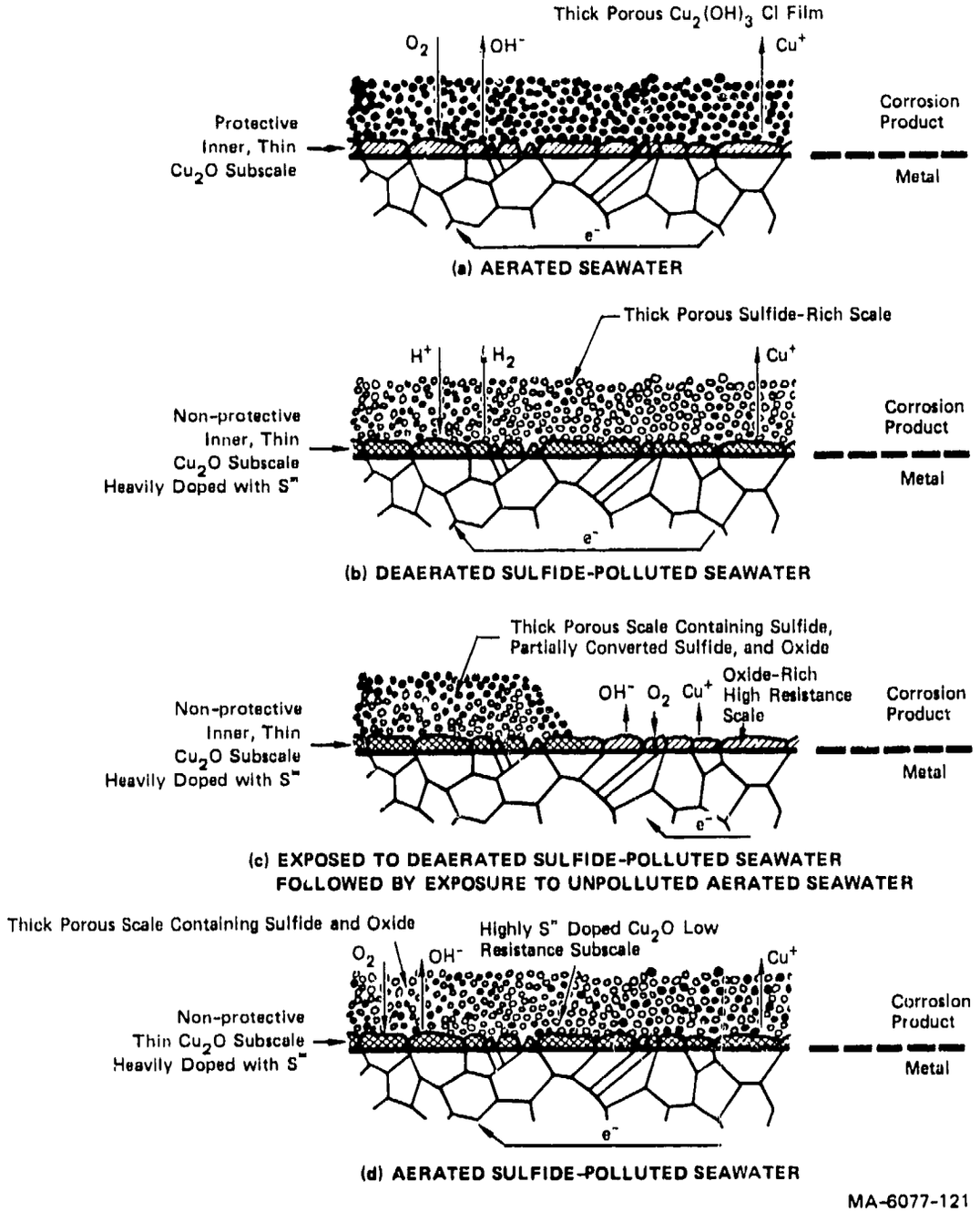

FIGURE 18 PROPOSED MECHANISM FOR THE ACCELERATED CORROSION OF COPPER/NICKEL ALLOY IN AERATED SULFIDE-POLLUTED SEAWATER

sulfur. Unlike the Cu/Ni alloys exposed to aerated seawater, the inner oxide layer is nonprotective because it contains cracks and other defects. This means that the anodic and cathodic processes are not separated by an IR drop, and both occur at the metal/inner corrosion product interface. The anodic process is Cu^{+} ion formation, and in complete absence of oxygen, the cathodic reaction is hydrogen ion reduction. If a limited amount of oxygen is present, the reduction of oxygen may be the dominant cathodic reaction. Since so few oxygen or hydrogen ions are available for the cathodic process, the overall corrosion process occurs relatively slowly and results in only slightly higher corrosion rates than those in aerated seawater. Therefore, the key to understanding the corrosion behavior in deaerated, sulfide-polluted seawater is the formation of a cracked, nonprotective Cu_2O/Cu_2S corrosion film.

Figure 18(c) helps to explain how Cu/Ni alloys exposed to aerated unpolluted seawater corrode more quickly if they have been preexposed to sulfide. Preexposure to sulfide-polluted seawater, either oxygen-free or containing only a trace of oxygen, results in the formation of a cracked, nonprotective corrosion product as discussed above. When the preexposed specimen is then exposed to aerated, unpolluted seawater, the initial corrosion rate is high because the cathodic reaction switches from the reduction of a low concentration of either oxygen or hydrogen ions to the reduction of a high concentration of oxygen. This increase in the cathodic process results in an initially high corrosion rate. The corrosion rate of the preexposed sample remains high after initial exposure to aerated, unpolluted seawater because a protective film will not form immediately, even though large quantities of oxygen are available in the bulk seawater for oxide formation. A protective film will not form because of the presence of residual sulfide trapped in the porous corrosive film remaining from the sulfide preexposure. However, this sulfide is consumed by the mechanisms discussed in Section IV. As the sulfide is consumed, the anodic redox potential is shifted to more noble values, and there is a transition from active to passive behavior, resulting in an eventual lowering the of corrosion rate. This effect of sulfide preexposure helps to explain how sulfide-polluted seawater can accelerate corrosion of Cu/Ni alloys.

The most noticeable corrosion acceleration effect is that brought about by the simultaneous exposure of Cu/Ni alloys to sulfide and oxygen. This behavior is illustrated in Figure 18(d). Since the cathodic redox potential is high and the anodic redox potential is low and since sulfide prevents the formation of a protective oxide, the corrosion rate is very high upon initial exposure to aerated, sulfide-polluted seawater. The rate remains high as long as sulfide and oxygen are present. Therefore, simultaneous exposure to sulfide and oxygen is most likely the cause of the observed accelerated attack of Cu/Ni alloys in sulfide-polluted seawater.

VI RECOMMENDATIONS FOR FUTURE RESEARCH

As this report indicates, considerable progress has been made toward understanding the corrosion mechanism of copper/nickel alloys in unpolluted and sulfide-polluted seawater. However, the present level of understanding is still primarily qualitative and provides little help in developing specific methods for protecting copper alloys from corrosion in polluted or unpolluted seawater environments.

Ideally, the level of understanding should be sufficient to permit design of better alloys, develop better inhibitors, and select optimum conditions for cathodically protecting components. It is not possible to accomplish any of these goals at present. However, further research to answer certain key questions could provide sufficient understanding to achieve many of these goals. We, therefore, recommend that the following subjects be studied in detail in future research programs.

- The structure and composition profiles of corrosion films formed on specimens exposed to flowing, polluted and unpolluted natural seawater need to be thoroughly studied using surface analysis tools such as Auger and ESCA. The present study has indicated that passivation of copper/nickel alloys can occur by the formation of a protective copper oxide layer that is doped with small amounts of iron, nickel, and chlorine. Bockris, Reddy, and Rao,[35] however, have suggested that the passivation behavior of nickel alloys is due to the formation of a protective nickel oxide layer. The few quantitative compositional profiles that have been measured on the corrosion products of copper/nickel alloys were limited to specimens exposed to artificial seawater.[7,36] These data seem to indicate that, if nickel enrichment occurs, it is limited to an outer, nonprotective corrosion film. Our own limited Auger data indicate that little nickel enrichment occurs in either the inner or outer corrosion films of copper/nickel alloys exposed to flowing, natural seawater. Nonetheless, the work to date on the composition of copper/nickel corrosion products is not definitive enough to rule out the previously proposed nickel oxide model. If this model is correct, then the work of Oudar and Marcus[37] on the effect of sulfide on passivation of nickel and nickel/iron

alloys could have some bearing on the corrosion of copper/nickel alloys in a polluted seawater environment. Oudar and Marcus found that passivation can occur only if the sulfur concentration on the surface is below the monolayer coverage.

- More detailed data on the composition profiles of corrosion products on copper/nickel alloys could indicate why small iron additions to these alloys improve their corrosion resistance.

- Preliminary work at SRI has shown that various sulfur species can cause accelerated attack of copper/nickel alloys. However, more research is needed to determine precisely which species are the most harmful. This information can help to determine what inhibitors or other types of water treatments can be used to control this accelerated attack. The effect of these species on the corrosion behavior of these copper/nickel alloys can easily be determined using the rotating ring disk electrode method or SRI's recently developed rotating cylinder-collector electrode.[38] In these methods, the hydrodynamics of fluid flow are well characterized; thus, the effect of seawater velocity on the corrosion behavior can be easily simulated.

- There is clearly a need to improve the accuracy of electrochemical methods for measuring corrosion rates in copper/nickel alloys. This requires that the Tafel coefficients, the polarization resistance, and the concentration and type of species taking part in the corrosion process be measured more accurately. Improved accuracy, which can be achieved by using AC impedance and rotating ring disk electrode methods, would allow the development of a method for making rapid, in-situ measurements on seawater condense tubing.

- The effects of low temperature heat treatments (200° to 350°C) on the corrosion behavior of copper/nickel alloys need to be investigated in some detail. Such heat treatments may be important because copper/nickel alloys undergo a phase separation in this temperature range,[39,40] and two-phase materials usually corrode faster than single-phase materials. Also, surface segregation of nickel or copper (which of these elements segregates to the surface depends on the environment the surface is exposed to) has been observed in these alloys after low temperature heat treatments.[39-40] It is not clear whether such segregation will improve or degrade corrosion resistance.

- The model for corrosion of copper/nickel alloys in seawater presented in this report needs to be quantified so that corrosion rates can be predicted as a function of exposure time and environment.

REFERENCES

1. J. P. Gudas and H. P. Hack, Corrosion, Vol. 35, No. 6, pp. 259-264 (1979).

2. H. P. Hack and J. P. Gudas, Materials Performance, pp. 25-28 (March 1979).

3. R. F. North and M. J. Pryor, Corrosion Science, Vol. 10, pp. 297-311 (1970).

4. H. H. Uhlig, Trans. Electrochem. Soc., Vol. 85, p. 307 (1944).

5. W. C. Stewart and F. L. LaQue, Corrosion, Vol. 8, p. 259 (1952).

6. J. M. Popplewell, R. J. Hart, and J. A. Ford, Corrosion Science, Vol. 13. p. 295 (1973).

7. C. Kato, J. E. Castle, B. G. Ateya, and H. W. Pickering, J. Electrochem. Soc., Vol. 127, No. 9, pp. 1897-1903 (1980).

8. J. M. Popplewell, NACE Corrosion/78, Houston, Texas, paper No. 21 (1978).

9. E. D. Mor and A. M. Beccaria, Br. Corr. J., Vol. 10, p. 33 (1975).

10. G. D. Bengough and R. May, J. Inst. Metals, Vol. 32, p. 200 (1924).

11. E. D. Mor and A. M. Beccaria, Corrosion, Vol. 30, No. 10, pp. 354-356 (1974).

12. J. F. Bates and J. M. Popplewell, Corrosion, Vol. 31, No. 8, pp. 269-275 (1975).

13. B. C. Syrett, "The Mechanism of Accelerated Corrosion of Copper-Nickel Alloys in Sulphide Polluted Seawater," Corrosion Science, to be published.

14. D. D. Macdonald, B. C. Syrett, and S. S. Wing, Corrosion, Vol. 35, p. 367 (1979).

15. B. C. Syrett, D. D. Macdonald, and S. S. Wing, Corrosion, Vol. 35, p. 409 (1979).

16. B. C. Syrett and D. D. Macdonald, Corrosion, Vol. 35, p. 505 (1979).

17. B. C. Syrett and S. S. Wing, Corrosion, Vol. 36, p. 73 (1980).

18. D. D. Macdonald, B. C. Syrett, and S. S. Wing, Annual Report to ONR, N00014-77-C-0046, NR036-116 (February 1979).

19. B. C. Syrett, S. S. Wing and D. D. Macdonald, Annual Report to ONR, N00014-77-C-0046, NR036-116 (February 1979).

20. D. D. Macdonald, B. C. Syrett, and S. S. Wing, Corrosion, Vol. 34, p. 278 (1978).

21. R. B. Niederberger and J. M. Popplewell, Corrosion/76, Houston, Texas paper, No. 76 (1976).

22. Standard Methods for the Examination of Water and Wastewater Including Bottom Sediments and Sludges, 12th ed. (American Public Health Assoc., New York, 1965).

23. M. Stern and A. L. Geary, J. Electrochem. Soc., Vol. 104, No. 1 (January 1957).

24. 1979 Annual Book of ASTM Standards, Part 10, American Society for Testing and Materials, Philadelphia, PA, pp. 722-734.

25. D. D. Macdonald, Transient Technique in Electrochemistry (Plenum Publishing Co. New York, 1977).

26. K. B. Oldham and F. Mansfeld, Corrosion, Vol. 27, P. 434 (1971).

27. Corrosion, Vol. 2, L. L. Shreir, Ed. (Nennes-Butterworths, London, 1976).

28. D. D. Macdonald, J. Electrochem. Soc., Vol. 125, p. 1443 (1978).

29. O. Kubaschewski and B. Hopkins, Oxidation of Metals and Alloys, 2nd Ed. (Butterworths, London, 1962).

30. R. S. Toth et al., Phys. Rev., Vol. 122, p. 482 (1961).

31. C. Wagner and H. Hammen, Z. Phys. Chem., Vol. 1340, p. 197 (1938).

32. F. A. Kröger, The Chemistry of Imperfect Crystals (North-Holland Publishing Company, Amsterdam, 1964).

33. M. O'Keeffe and W. J. Moore, J. Chem. Phys., Vol. 35, p. 1324 (1961).

34. E. D. Verink Electrochemical Techniques for Corrosion, R. Baboian, Ed. (NACE, Houston, Texas, 1977), p. 43.

35. J. O'M. Bockris, A.K.N. Reddy, and B. Rao, J. Electrochem. Soc., Vol. 113, p. 1133 (1966).

36. G. E. McGuire, A. L. Bacarella, J. C. Griess, Jr., R. E. Clausing, and L. D. Hulett, J. Electrochem. Soc., Vol. 125, No. 11, pp. 1801-1804, (1978).

37. J. Oudar and P. Marcus, Applications of Surface Science, Vol. 3, P. 48-67 (1979).

38. M.C.H. McKubre and D. D. Macdonald, J. Electrochem. Soc., Vol. 127, No. 3, P. 633, (1980).

39. W.M.H. Sachtler and P. Van Der Plank, Surface Science, Vol. 18, P. 62 (1969).

40. D. T. Ling, J. N. Miller, I. Lindau, W. E. Spicer, and P. M. Stefan, Surface Science, Vol. 74, P. 612 (1978).

41. T. T. Tsong, Y. S. Ng, and S. B. McLane, Jr., J. Appl. Phys., Vol. 51, No. 12, P. 6189 (1980).

Appendix

DERIVATION OF CORROSION CURRENT AS A FUNCTION OF POLARIZATION RESISTANCE

To obtain the relationship between the corrosion rate and the polarization resistance of the corroding interface one needs to develop the potential/current relationship for the interface.

The net current, i, at a given potential difference, E, between the local anodes and cathodes on the corroding interface can be written:

$$i = \overleftarrow{i}_1 - \overrightarrow{i}_1 + \overleftarrow{i}_2 - \overrightarrow{i}_2 \tag{A1}$$

where: $\overleftarrow{i}_1$ = anodic current for metal dissolution

$\overrightarrow{i}_1$ = anodic current for metal deposition

$\overrightarrow{i}_2$ = cathodic current for reduction of the cathodic reactant

$\overleftarrow{i}_2$ = cathodic current for oxidation of the cathodic reactant

The anodic current $\overleftarrow{i}_1$ and the cathodic $\overrightarrow{i}_2$ can be expressed as:

$$\overleftarrow{i}_1 = A_1 \, i_{0,1} \exp\left[\frac{E - E_{0,1}}{\overleftarrow{\lambda}_1}\right] \tag{A2}$$

and

$$\overrightarrow{i}_2 = A_2 \, i_{0,2} \exp\left[\frac{E_{0,2} - E}{\overrightarrow{\lambda}_2}\right] \tag{A3}$$

where: A_1 = anodic area

A_2 = cathodic area

$i_{0,1}$ = exchange current density for the anodic process

$i_{0,2}$ = exchange current density for the cathodic process

$E_{0,1}$ = reversible potential for anodic dissolution

$E_{0,2}$ = reversible potential for cathodic reduction

$\overleftarrow{\lambda}_1$ = anodic Tafel slope

$\overrightarrow{\lambda}_2$ = cathodic Tafel slope

Although similar expressions can be written for $\overrightarrow{i}_1$ and $\overleftarrow{i}_2$, they can be neglected in this development since the potential is considered far from either $E_{0,1}$ or $E_{0,2}$. This makes $\overrightarrow{i}_1$ and $\overleftarrow{i}_2$ and their contribution to the total current, equation (A1) negligible. Hence substituting equations (A2) and (A3) into equation (A1):

$$i = A_1 i_{0,1} \exp\left[\frac{E - E_{0,1}}{\overleftarrow{\lambda}_1}\right] - A_2 i_{0,2} \exp\left[\frac{E_{0,2} - E}{\overrightarrow{\lambda}_2}\right] \qquad \text{(A4)}$$

At the corrosion potential, E_c, the net current is zero since $\overleftarrow{i}_1 = \overrightarrow{i}_2$. The corrosion current, i_c, equals $\overleftarrow{i}_1$ and, therefore,

$$i_c = A_1 i_{0,1} \exp\left[\frac{E_c - E_{0,1}}{\overleftarrow{\lambda}_1}\right] = A_2 i_{0,2} \exp\left[\frac{E_{0,2} - E_c}{\overrightarrow{\lambda}_2}\right] \qquad \text{(A5)}$$

To obtain the relationship between the polarization resistance and the corrosion current, differentiating equation (A4) with respect to E gives:

$$\left(\frac{di}{dE}\right)_{E_c} = 1/R_p = \frac{A_1 i_{0,1}}{\overleftarrow{\lambda}_1} \exp\left[\frac{E_c - E_{0,1}}{\overleftarrow{\lambda}_1}\right] + \frac{A_2 i_{0,2}}{\overrightarrow{\lambda}_2} \exp\left[\frac{E_{0,2} - E_c}{\overrightarrow{\lambda}_2}\right] \qquad \text{(A6)}$$

where R_p is the polarization resistance.

Combining equations (A5) and (A6) gives the Stern-Geary equation* relating corrosion current to the polarization resistance

$$i_c = (1/R_p)\left(\frac{\vec{\lambda}_1\vec{\lambda}_2}{\vec{\lambda}_1 + \vec{\lambda}_2}\right) \tag{A7}$$

The weight loss caused by corrosion can be calculated by integration equation (A7) to obtain the charge transfer and then applying Faraday's law. Assuming that the Tafel coefficients for the partial anodic and cathodic reactions are time independent, the charge associated with metal loss, Q_c, is

$$Q_c = \frac{\lambda_1\lambda_2}{\lambda_1 + \lambda_2}\int_0^t R_p^{-1}\, dt \tag{A8}$$

Application of Faraday's law gives the weight loss from corrosion (ΔW) as:

$$\Delta W = \frac{-\bar{M}\, Q_c}{\bar{n}F} \tag{A9}$$

or the instantaneous corrosion rate (dW/dt) as:

$$dW/dt = \frac{-\bar{M}}{\bar{n}F}\, i_c \tag{A10}$$

where the composition averaged atomic weight, $\bar{M}$, and the average change in oxidation state, $\bar{n}$, are given by:

$$\bar{M} = X_{Cu}\, M_{Cu} + X_{Ni}\, M_{Ni} \tag{A11}$$

*M. Stern and A. L. Geary, J. Electrochem. Soc., Vol. 104, No. 1 (January 1957).

and

$$\bar{n} = X_{Cu} + 2X_{Ni} \qquad \text{(A12)}$$

and F = Faraday's constant.

In equations (A10) and (A11), X_{Cu} and X_{Ni} are the mole fractions of copper and nickel in the alloy. Furthermore, it is assumed that these components are oxidized to the +1 (cuprous) and +2 (nickelous) states, respectively, and that the average change oxidation states or the composition averaged atomic weight do not change with time.

TECHNICAL PAPERS PUBLISHED DURING ONR CONTRACT
N0014-77-C-0046, NR036-116

1. D. D. MacDonald, B. C. Syrett, and S. S. Wing, "The Corrosion of Copper-Nickel Alloys 706 and 715 in Flowing Seawater. I: Effect of Oxygen," Corrosion, Vol. 34, p. 289 (1978).

2. D. D. MacDonald, "An Impedance Interpretation of Small Amplitude Cyclic Voltammetry. I: Theoretical Analysis for a Resistive-Capacative System," Journal of the Electrochemical Society, Vol. 125, p. 1443 (1978).

3. D. D. MacDonald, "An Impedance Interpretation of Small Amplitude Cyclic Voltammetry. II: Theoretical Analysis of Systems that Exhibit Pseudoinductive Behavior," Journal of the Electrochemical Society, Vol. 125, p. 1977 (1978).

4. D. D. MacDonald, "A Method for Estimating Impedance Parameters for Electrochemical Systems that Exhibit Pseudoinductance," Journal of the Electrochemical Society, Vol. 125, p. 2062 (1978).

5. D. D. MacDonald, B. C. Syrett, and S. S. Wing, "The Corrosion of Copper-Nickel Alloys 706 and 715 in Flowing Seawater. II: Effect of Dissolved Sulfide," Corrosion, Vol 35, p. 367 (1979).

6. B. C. Syrett, D. D. MacDonald, and S. S. Wing. "Corrosion of Copper-Nickel Alloys in Seawater Polluted with Sulfide and Sulfide Oxidation Products," Corrosion, Vol. 35, p. 409 (1979).

7. B. C. Syrett and S. S. Wing, "Effect of Flow on Corrosion of Copper-Nickel Alloys in Aerated Seawater and in Sulfide-Polluted Seawater," Corrosion, Vol. 36, p. 73 (1980).

8. B. C. Syrett, "The Mechanism of Accelerated Corrosion of Copper-Nickel Alloys in Sulfide-Polluted Seawater," accepted for publication in Corrosion Science (1980).

TECHNICAL REPORTS WRITTEN DURING ONR CONTRACT
N0014-77-C-046, NR036-116

1. D. D. MacDonald, B. C. Syrett, and S. S. Wing, "A Study to Determine the Mechanism of Corrosion of Copper-Nickel Alloys in Sulfide-Polluted Seawater," Annual Report to Office of Naval Research, Contract No. N00014-77-C-0046 (February 1978).

2. D. D. MacDonald, B. C. Syrett, and S. S. Wing, "A Study to Determine the Mechanisms of Corrosion of Copper-Nickel Alloys in Sulfide-Polluted Seawater," Annual Report to Office of Naval Research, Contract No. N00014-77-C-0046, NR03-116 (February 1979).